Present and future synoptic circulation patterns associated with cold and snowy spells over Italy

Miriam D'Errico[1,*], Flavio Pons[1,*], Pascal Yiou[1], Soulivanh Tao[1], Cesare Nardini[2], Frank Lunkeit[3], and Davide Faranda [1,4,5]

[1]Laboratoire des Sciences du Climat et de l'Environnement, UMR 8212 CEA-CNRS-UVSQ, Université Paris-Saclay, IPSL, 91191 Gif-sur-Yvette cedex, France
[2]Service de Physique de l'État Condensé, CNRS UMR 3680, CEA-Saclay, 91191 Gif-sur-Yvette, France
[3]Meteorological Institute, CEN, University of Hamburg, Bundesstrasse 55, 20146 Hamburg, Germany
[4]London Mathematical Laboratory, 8 Margravine Gardens London, W6 8RH, UK
[5]LMD/IPSL, Ecole Normale Superieure, PSL research University, Paris, France
[*]Equal Contributions

Correspondence: Davide Faranda (davide.faranda@lsce.ipsl.fr)

Abstract. Cold and snowy spells are compound extreme events with the potential of causing high socioeconomic impacts. Gaining insight on their dynamics in climate change scenarios could help anticipating the need for adaptation efforts. We focus on winter cold and snowy spells over Italy, reconstructing 32 major events in the past 60 years from documentary sources. Despite warmer winter temperatures, very recent cold spells have been associated to abundant, and sometimes exceptional snowfall. Our goal is to analyse the dynamical weather patterns associated to these events, and understand whether those patterns would be more or less recurrent in different emission scenarios using an intermediate complexity model (PlaSim). Our results, obtained by considering RCP2.6, RCP4.5 and RCP8.5 end-of-century ~~CO2~~ equivalent CO_2 concentrations, suggest that the likelihood of ~~analogous synoptic configurations of these~~ synoptic configurations analogous to those leading to extreme cold spells would grow substantially under increased emissions.

1 Introduction

Cold and snowy spells are driven by the mid-latitude atmospheric circulation through the amplification of planetary waves (Tibaldi and Buzzi, 1983; Barnes et al., 2014; Lehmann and Coumou, 2015), while they are sustained by thermodynamic effects occurring at local scales (e.g. presence of snow on the ground, availability of humidity) (Screen, 2017; WMO, 1966). Previous studies on current and future trends in the frequency and intensity of cold and snowy spells are not conclusive because of the disagreement in the definition of these events (Peings et al., 2013; Vavrus et al., 2006). If we consider separately cold spells and snowfalls, a large consensus is found in the literature: when focusing on cold spells events only, the Intergovernmental Panel on Climate Change (IPCC) fifth assessment report (Pachauri et al., 2014, Working Group 1, Chapter 4) ~~points as "very likely" a decrease of~~ describes the decrease in number of ice days and low ~~temperatures~~temperature days as "very likely". Indeed, there is also a large consensus that average snowfall and snow-cover are decreasing in the Northern Hemisphere (Liu et al., 2012; Brown and Mote, 2009; Faranda, 2020). These trends have been observed also for Italy, as reported in several

studies. The decrease in average snowfall ~~on~~ in Northern Italy observed in the last decades has been linked to the increase of temperature due to global climate change (Asnaghi, 2014; Mercalli and Berro, 2003). Similar conclusions also hold for the Alpine region (Serquet et al., 2011; Nicolet et al., 2016, 2018)~~. For Central and Southern Italy,~~ , and several studies (Diodato, 1995; Mangianti and Beltrano, 1991) also confirm these trends for Central and Southern Italy. On a more general basis, the study ~~of~~ by Diodato et al. (2019) shows that the variability of average snowfall over Italy ~~for~~ during the past millennium can be connected to ~~the~~ changes in temperature, with periods of abundant average snowfalls corresponding to generally colder periods (e.g. the little Ice Age) and warmer periods yielding limited snow accumulations. These negative trends on average snowfall are also expected in future warmer climate emission scenarios (Pachauri et al., 2014, Working Group 1, Chapter 4).

In this study, we focus on the dynamics of compound extreme cold and snowy events, for which the response to mean global change might be different from that of the individual variables (temperature and snowfall). Indeed, taking this complementary compound extreme events point of view (Zscheischler et al., 2020), some authors have found complex interactions between thermodynamic and dynamical processes when cold and snowy spells occur ~~(Deser et al., 2017; Overland and Wang, 2010; Strong et al., 20~~ (Easterling et al., 2000; Strong et al., 2009; Overland and Wang, 2010; Wu and Zhang, 2010; Marty and Blanchet, 2012; Coumou and Rah . In particular, warmer surface and sea surface temperatures can enhance convective snowfall precipitations under specific conditions and over regions with a large availability of moisture, such as the great Lakes in the US, Japan and Mediterranean countries (Steiger et al., 2009; Murakami et al., 1994). For Japan, Kawase et al. (2016) have shown that the interaction ~~of the Japan Sea~~ between the Sea of Japan polar air mass convergence zone ~~with the~~ and topography may enhance extreme snowfalls in future climates via a thermodynamic feedback. More recently, Faranda (2020) has analysed the trends in snowfall in Europe and observed that, in some countries, large snowfall amounts in the recent decades can be associated to a modification in the large scale atmospheric patterns driving these events. ~~Those~~ Concerning trends in extreme snowfall at the global level, O'Gorman (2014) used an ensemble of global climate simulations to show that, while average daily snowfall will experience a marked decline with global warming, only very small fractional changes are expected to affect daily snowfall extremes. These analyses raise a number of questions: does ~~the~~ anthropogenic forcing affect the frequency and/or intensity of this kind of compound events? How does the large-scale atmospheric dynamics impact ~~cold spell~~ cold spell events? Will local feedbacks (i.e. warm sea-surface temperatures enhancing convective snow precipitations) play a role in increasing cold spells hazards?

In this paper, we focus specifically on Italy: recent cold and snowy spells in this country have caused casualties in the population, strongly affected ground and air transportation and caused disruptions in services (meteogiornale.it, last access: 26/07/2020; ansa.it, last access: 26/07/2020). Our strategy to tackle these questions is to analyse simulations produced in a Global Circulation Model (GCM) under different emission scenarios. We first validate the cold and snowy spells produced ~~in~~ by a simplified GCM of intermediate complexity with historical forcing, i.e. the Planet Simulator (PlaSim) (Fraedrich et al., 2005a, b) against those detected in a reanalysis dataset. Then we analyse dynamic analogues of cold and snowy spell events under different climate change scenarios. This work is structured as follows: in Section ~~??~~2, we present sources and datasets used for the detection of compound cold and snow events over Italy. Simulation results obtained with Plasim GCM are presented in Section ~~3.~~ 3. We discuss our findings and give an outlook for future studies in ~~Section 4.~~ 4.

2 ~~Cold-spells definition and detection of analogues~~

2 cold spells definition and detection of analogues

2.1 Sources and data-set

Our study is based on the detection of synoptic meteorological configurations ~~likely linked~~ leading to cold spells over Italy in PlaSim, considering a control run based on ~~present-day climate, a run involving increased SST to evaluate the thermodynamic role of the ocean,~~ the recent historical climate and a set of ~~thee increased CO_2~~ three increased emission scenarios at the steady state. In order to do so, we will proceed with the following steps:

1. identify large scale, high impact winter cold spells over Italy;
2. describe the dynamic and thermodynamic conditions associated to such cold spells;
3. detect cold spell analogues in a historical climate dataset;
4. detect cold spell analogues in PlaSim runs, and evaluate if climate change can significantly modify their frequency, and in which direction;
5. characterize the PlaSim cold spell analogues in analogy to point 2, to assess the potential of the considered dynamic ~~configuration~~ configurations in producing relevant winter phenomena in a sensibly warmer climate.

In order to identify relevant cold spells over Italy, we consider documented events that have produced at least a record low temperature and/or a record snowfall amount (or snow at locations where snowfall has never been previously reported) at one or more locations in Italy. We combine official sources and both professional and avocational websites dedicated to weather and climate, where collections of weather event reports are available, and we counter-check their validity with station data and trusted documentary sources (Bailey, 1994; Payne and Payne, 2004). Our documentary sources include local networks, newspapers and periodicals (see ~~Section~~ Appendix A); news and commercial meteorological websites [ansa.it; meteo net; meteolanguedoc.com; 3bmeteo.com; meteociel.fr; meteogiornale.it]; temperature and hydrological records [evalmet.it, Servizio Idrografico e Mareografico Nazionale].

The in-depth description of the effects of each cold spell at the country level is presented in Appendix A. Here, we provide a general picture of the typical event through a local analysis focused on the cities of Bologna and Campobasso. The former stands at the Southern edge of the Po Valley, at the foot of the North-Eastern Appenninic range; the latter is located in the Southern Appennini, at about 45 km from the closest Adriatic coast and 85 km from the closest Tyrrhenian coast. Due to their ~~positions~~position, both cities are exposed to snowfall in case of cold spells characterized by either cold air flowing directly from the East, or by Mediterranean cyclogenesis. In the latter case, Arctic air reaches the Mediterranean Sea through the Rhone Valley ~~,~~ often after the formation of a cyclone leeward to the Alps ~~,~~ and hits the Eastern Italian coasts as ~~Sirroco~~ Sirocco and Bora winds, as the pressure minimum moves South. In both cases, snowfall on the two cities can be enhanced by the interaction of the Easterly low level winds drawing moisture from the Adriatic with the Appenninic range, due to

orographic ~~effects~~lift. Data for Bologna are provided by the local Regional Environment Protection Agency [https://www.arpae.it/documenti.asp?parolachiave=sim_annali&cerca=si&idlivello=64] and by Randi and Ghiselli (2013), while those used for Campobasso by [Servizio Idrografico e Mareografico di Pescara, https://www.regione.abruzzo.it/content/annali-idrologici; http://www.protezionecivile.molise.it/centro-funzionale/la-rete-meteo-idro-pluviometrica.html]. Figure 1 shows the amount of snowfall, the minimum temperature near the surface and the duration of each cold spell that are recorded in Campobasso and in Bologna between 1954 and 2018 from hydrological archives [www.arpae.it/documenti.asp].

Given the heterogeneous and, in some cases, unofficial origin of the considered data, we only aim at drawing a qualitative picture. Overall, our analysis indicates that extreme snowfalls have occurred in recent years, despite warming temperatures (Fig. 1a). For example, 50 cm to 60 cm snow ~~height was measured in~~ depth was measured on the bordering side of the coasts in Puglia and Marche during the January 2016 event, and a similar amount was recorded in the Campobasso area. The snowfall amounts do not seem ~~to yield~~ affected by decreasing trends, although it can be argued that the duration of the events slightly decreases and ~~their~~ the associated minimum temperatures slightly increase. In another study performed using reanalysis and observational data, Faranda (2020) performed yearly block maxima analyses of snowfalls over Europe, showing that contrasting trends appear for extreme snowfalls over Italian regions.

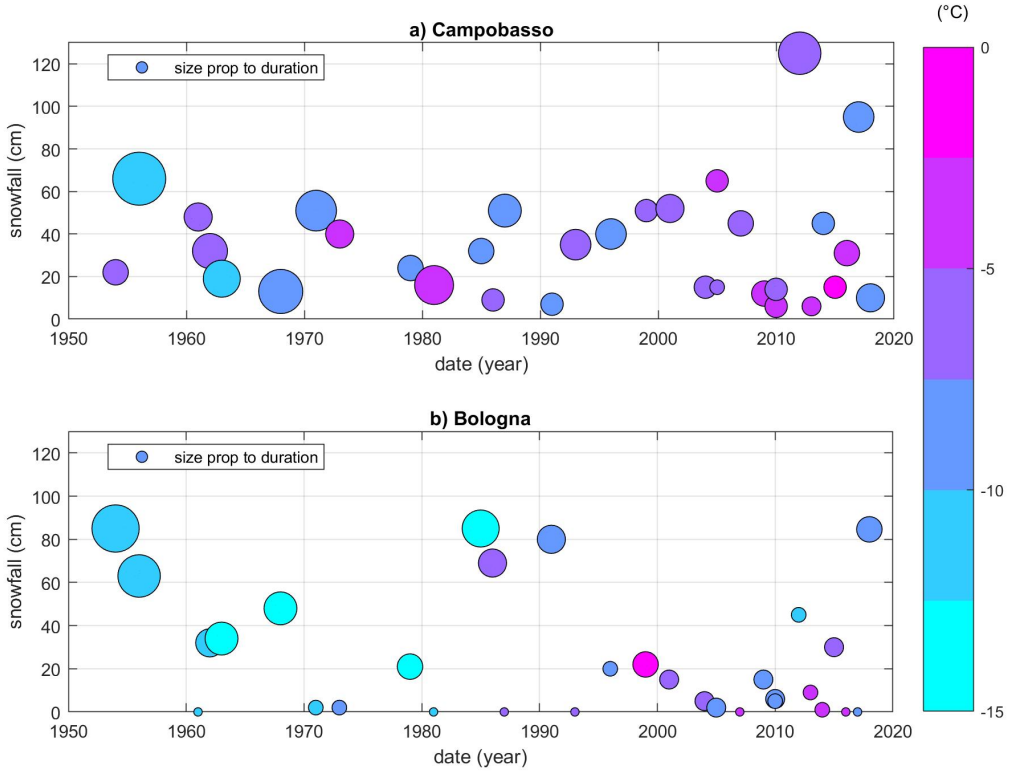

Figure 1. Cold spells from documentary sources. Data recorded in a) Campobasso (686 m of altitude); b) Bologna (54 m of altitude). Each ball represents one cold spell event. The ~~size~~ diameter is proportional to the number of snowfall days. The y-axis shows the snowfall measured during each event. The color shows the minimum near surface temperature recorded during the event (see Sources and data-set).

2.2 Observed Cold Spell Dynamics

Besides the qualitative analysis involving the cities of Bologna and Campobasso briefly presented in Section ??2, we now aim at characterizing the dynamic and thermodynamic features of the considered cold spells at the synoptic scale. To this purpose, we rely on the National Centers for Environmental Prediction (NCEPv2) Reanalysis dataset. In particular, we consider geopotential height at 500 hPa (Z500) and sea-level pressure (SLP) as dynamical fingerprints and to compute the analogues Jézéquel et al. (2018), temperature at 850 hPa (T850) to track cold air advection without surface disturbances (Grazzini, 2013), 2 meter temperature (T2M) to characterize near-surface conditions~~and the~~ , and daily precipitation rate (PRP).

Although our analysis is focused on cold spells affecting an area containing Italian borders, the dynamic determinants of such cold spells span much larger scales. For this reason, we consider a larger area, including Europe, European Russia, and the North Atlantic, over a 2.5 degree grid comprised between [22.5–70N, 80W–70E]. We first perform an unsupervised cluster analysis based on the Z500 standardized anomaly fields using a k-means algorithm (Michelangeli et al., 1995), and we inspect the Z500, SLP and T850 fields averaged over each cluster.

For Z500 and SLP, we consider standardized anomalies from the December-January-February-March (DJFM) climatology, ~~which includes~~ since these months include all the events described in Section A. Standardized anomalies are obtained by subtracting the DJFM mean and dividing by the DJFM standard deviation.

In order to ~~decide~~ choose the optimal number of clusters, we first performed a scree plot (not shown), obtained by plotting the within-groups sum of squared differences from the cluster ~~centroid~~centroids. This analysis did not give clear indications about the ideal number of clusters. Therefore, we compared clustering results at different values of k, finding that for $k = 3$ ~~2~~ two of the three clusters displayed very similar spatial features, and with larger k the resulting clusters can always be reduced to two main patterns: we then ~~decide to~~ choose $k = 2$. We remark that the k-means algorithm and other clustering techniques are based on assumptions such as equal size and sphericity of the clusters, which can be met only in coarse approximation in real-world high dimensional datasets. In particular, the poor indications from the scree plot may be due to the different number of events assigned to each cluster (respectively ~~18 and 14~~ 22 and 10 for $k = 2$). However, we find the results consistent enough to allow for a qualitative analysis.

In Fig. 2 we show the Z500 fields (a,b) ~~, the Z500 standardized anomalies (c,d),~~ and the SLP fields (e,f) averaged over the 18 events in cluster 1 (a,c~~,e~~) and cluster 2 (b,d~~,f)~~), and the corresponding standardized anomalies as red (positive) and black (negative) standardized anomalies. The dynamic configurations in the two clusters differ deeply, suggesting the existence of at least two typical large scale cold spell drivers.

Cluster 1 ~~is characterized by an Omega wavy structure associated to an Atlantic high-pressure ridge (Falkena et al., 2020; Faranda, 2020) reaching South of Iceland and a trough embracing Italy and the Balkans. A trough of low Z500 values is also present over the North Atlantic, between the Azores and North America. The SLP field presents a similar structure, with~~ presents a ~~high pressure system located over the United Kingdom and a deep low anomaly centered over Southern Italy and Greece. In such a situation, cold air is drawn from the North by the Mediterranean cyclone, flowing from Scandinavia over Central-Western Europe and entering the Mediterranean from the Rhone Valley and the Gulf of Trieste due to the presence of the Alps.~~

~~Cluster 2 presents a Scandinavian blocking pattern~~pattern resembling a Scandinavian blocking, but with a positive SLP anomalies displaced to the South, with an anticyclone stretching ~~zonally in a WSW-ENE~~ in a SW-NE direction, rather than elevating along the meridians, and low pressure values ~~again~~ centered over the Central Mediterranean, mainly confined below 40 degrees N. The axis of the anticyclone is located at about 50-60 degrees N, so that cold Arctic air is free to flow on its Southern edge in a ENE-WSW direction, drawn by the Mediterranean low, after assuming partially continental ~~characteristics while passing~~ features while streaming over Russia and Eastern Europe. In this situation, cold air easily reaches Central-Southern Italy after increasing its humidity content over the Adriatic Sea. This causes snowy precipitation bands to form slightly offshore the East Italian coast, which can be later amplified by the orographic effect caused by the Appenninic range, with abundant snowfall even at low altitudes (Stocchi and Davolio, 2017).

Cluster 2 is characterized by an Omega wavy structure associated to an Atlantic high-pressure ridge (Falkena et al., 2020; Faranda, 2020) reaching Iceland, and to a trough embracing Italy and the Balkans. A trough associated to low Z500 values is also present over the North Atlantic, between the Azores and North America. The SLP field presents a similar structure, with a high pressure system centered over the United Kingdom and a deep low anomaly centered over Southern Italy and Greece. In such a situation,

cold air is drawn from the North by the Mediterranean cyclone, flowing from Scandinavia over Central-Western Europe and entering the Mediterranean from the Rhone Valley and the Gulf of Trieste due to the presence of the Alps.

Fig. 3 shows the corresponding T850 (a,b), T2M (c,d) and PRP (e,f) fields. We begin with the analyses of T850 hPA fields: despite the sensibly different dynamic setting, the penetration of cold air into the Mediterranean is quite similar in the two clusters, with strong negative anomalies embracing the whole Central Mediterranean including the entire Italian peninsula. The main differences concern the UK, Iceland and Scandinavia, due to the ~~very~~ different direction of the high pressure axis. In cluster 1, the tilted high pressure drives warmer air towards the British Isles and Scandinavia, while the cold anomaly is confined to more Southern latitudes. In cluster 2, the meridionally oriented axis brings warmer air towards Greenland and Iceland, while the core of the cold air is located between Scandinavia and Central Europe. ~~In cluster 2, the tilted high pressure drives warmer air towards the British Isles and Scandinavia, while the cold anomaly is confined to more Southern latitudes.~~ The T2M fields (Fig. 3 c,d) show generally ~~above zero~~ above-zero temperatures over Central-Southern Italy during these events: this is partially due to the coarse resolution of the NCEPv2 dataset that considers Southern Italy and Sicily as sea grid points. Italy is also a country with a complex geography and mountain ranges (the Alps and the Apennines) extending from North to South. This causes a strong temperature gradient across the country. Indeed, for both clusters, the T850 temperatures shown in panels Fig. 3 (a,b) are sufficient to produce snowfall in the Po Valley, and at low altitudes on the hills and mountains of the country. Finally, the PRP fields (Fig. 3 e,f) show that these events are indeed associated with consistent precipitation amounts over ~~Italy and the Balkans, with second cluster producing large precipitations also over Sardinia.~~ Southern Italy and Sardinia (especially in cluster 1) and the Balkans (especially in cluster 2).

We measure the uncertainty associated to the cluster composites discussed above by computing the standard deviation of the standardized anomalies used for the clustering, shown in figures 4 and 5. Low uncertainty is overall associated to the position of Z500 maxima and minima driving the cold spells in both clusters. Small values of the SLP standard deviation are also associated to low-level high and low pressure systems in cluster 1, while the position of the low pressure on the Eastern Mediterranean in cluster 2 is affected by the high uncertainty. Concerning temperature, high (cluster 1) and very high (cluster 2) uncertainty is attributed to the position of Western limit of the cold pool of air at 850 hPa (see panels (a) and (b) of figure 5), and high uncertainty affects the penetration of cold air into the Mediterranean area at the low levels (panels (c) and (d)).

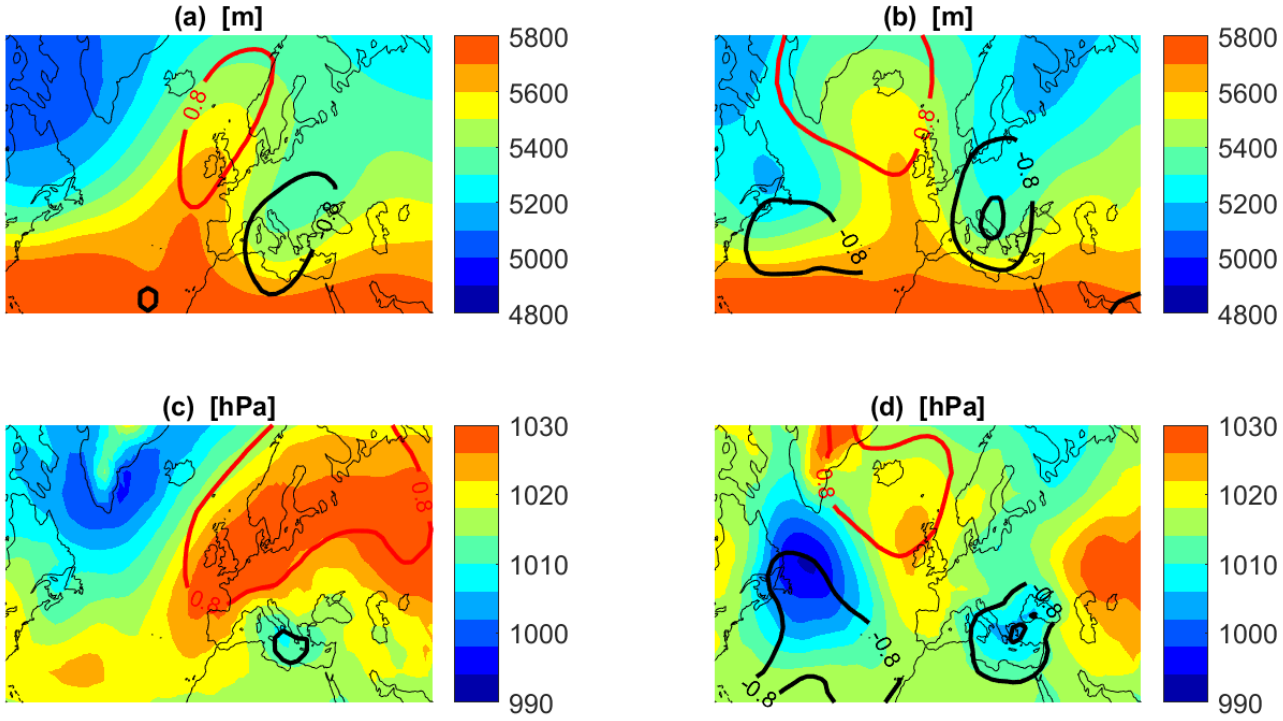

Figure 2. ~~**Dynamics for clusters of cold-spells over Italy**~~ **Dynamics for clusters of cold spells over Italy** 500 hPa Geopotential height [m] (a,b) ~~with associated standardized anomalies (c,d)~~ and sea-level pressure [hPa] (~~e~~c,~~f~~d) averaged over the two clusters of ~~cold-spells~~ cold spells in Italy found via ~~k-means~~*k*-means. Cluster 1 (a,c,~~e~~) is characterized by ~~an omega-blocking pattern~~ a zonally tilted high pressure located between the ~~Atlantic~~ British Islands and ~~Europe~~Russia, cluster 2 (b,d,~~f~~) by ~~a zonally tilted high pressure located~~ an omega-blocking pattern between the ~~British Islands~~ Atlantic and ~~Russia~~Europe. Black and red isolines represent negative and positive standardized anomalies.

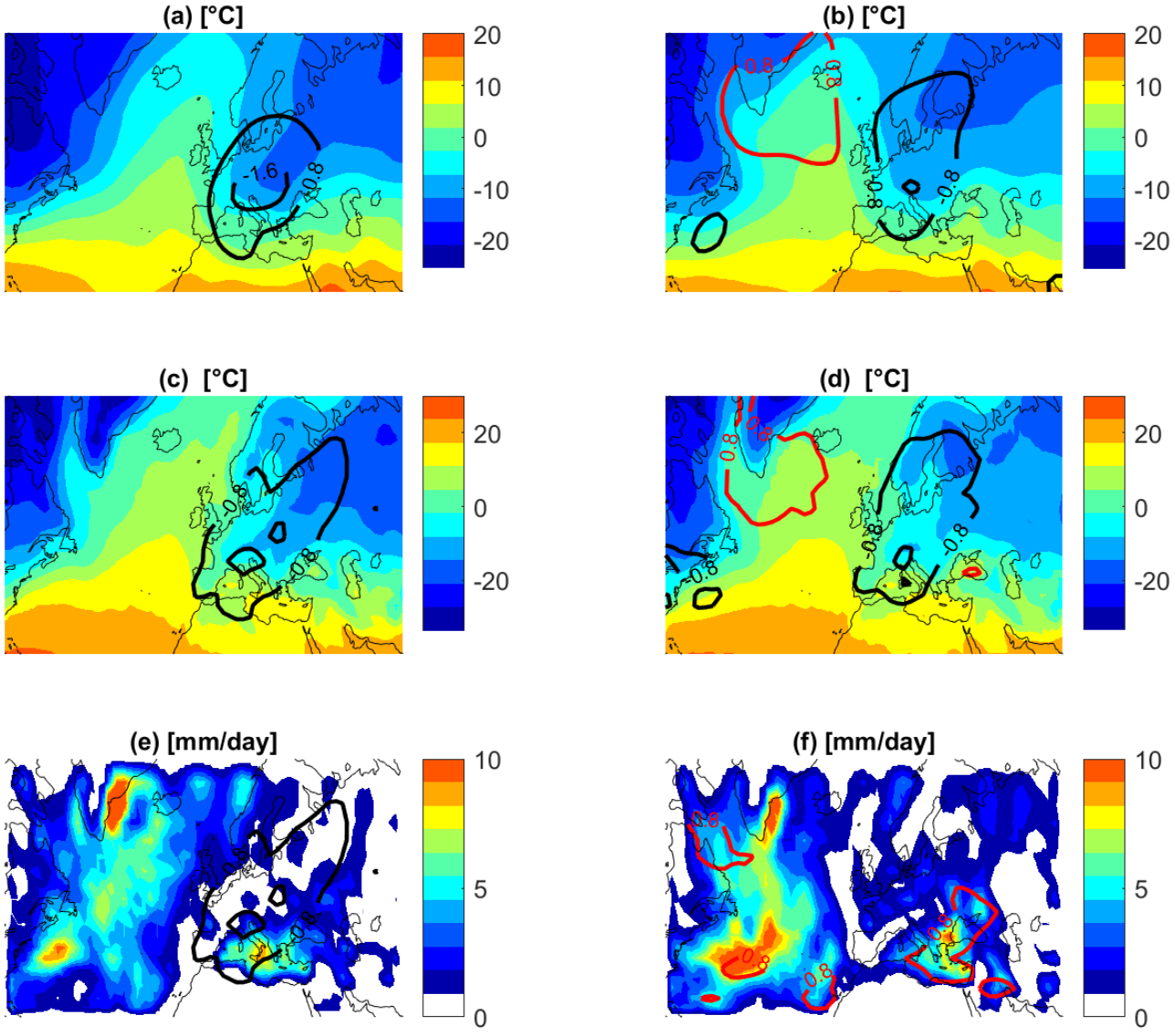

Figure 3. ~~**Physics for clusters of cold-spells over Italy**~~ **Physics for clusters of cold spells over Italy** Temperature at 850 hPa [°C] (a,b), two meters temperatures [°C] (c,d), precipitation rate [mm/day] (e,f) averaged over the two clusters of ~~cold-spells~~ cold spells in Italy found via ~~k-means~~*k*-means. In cluster 1 (a,c,e) warm air ~~extends North from~~ is advected towards the ~~Azores to Iceland~~ British Islands and cold air flows ~~South~~ mainly from ~~Scandinavia~~Russia and Eastern Europe. In cluster 2 (b,d,f) warm air ~~is advected towards~~ extends North from the ~~British Islands~~ Azores to Iceland and cold air flows ~~mainly~~ South from ~~Russia and Eastern Europe~~Scandinavia. The temperature field at the surface is very similar, with cold temperatures over continental areas, and negative or very low positive daily values over Italy, especially the peninsular regions. Black and red isolines represent negative and positive standardized anomalies.

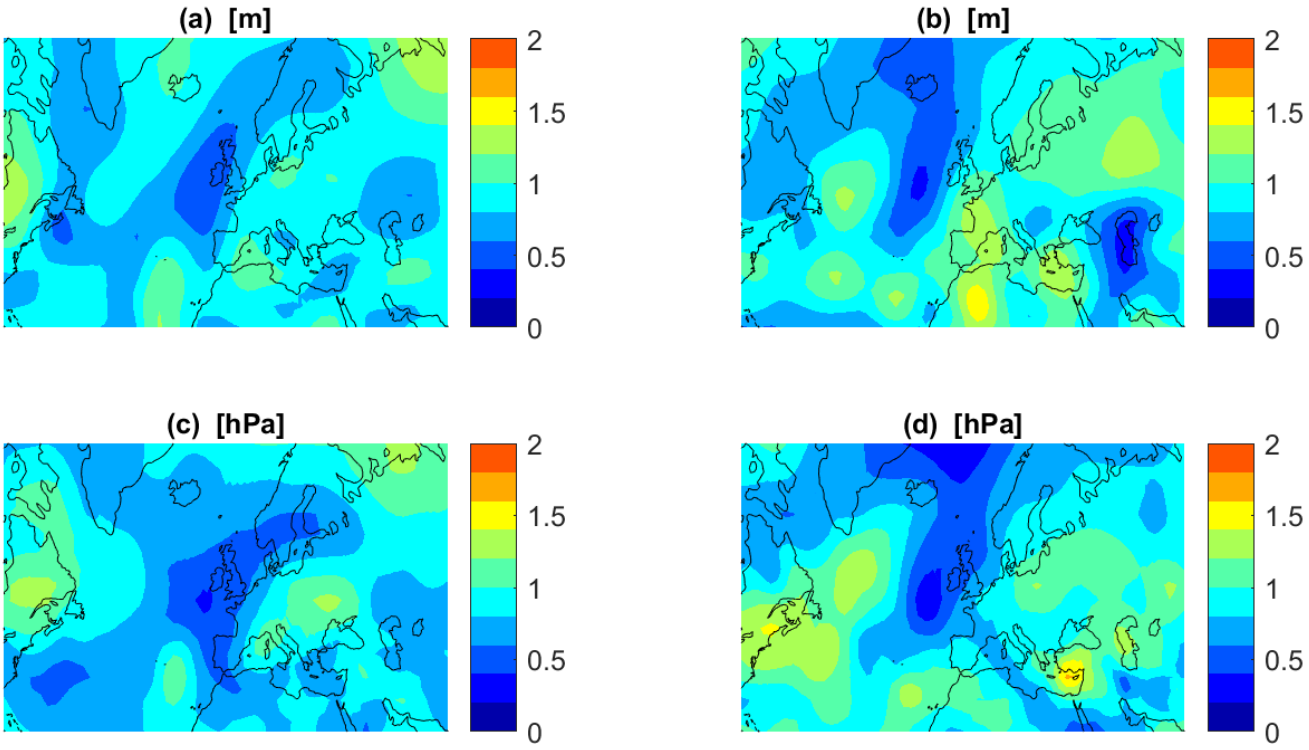

Figure 4. **Cluster uncertainty** Standard deviation of 500 hPa Geopotential height [m] (a,b) and sea-level pressure [hPa] (e,f) of the two clusters of cold spells in Italy found via k-means.

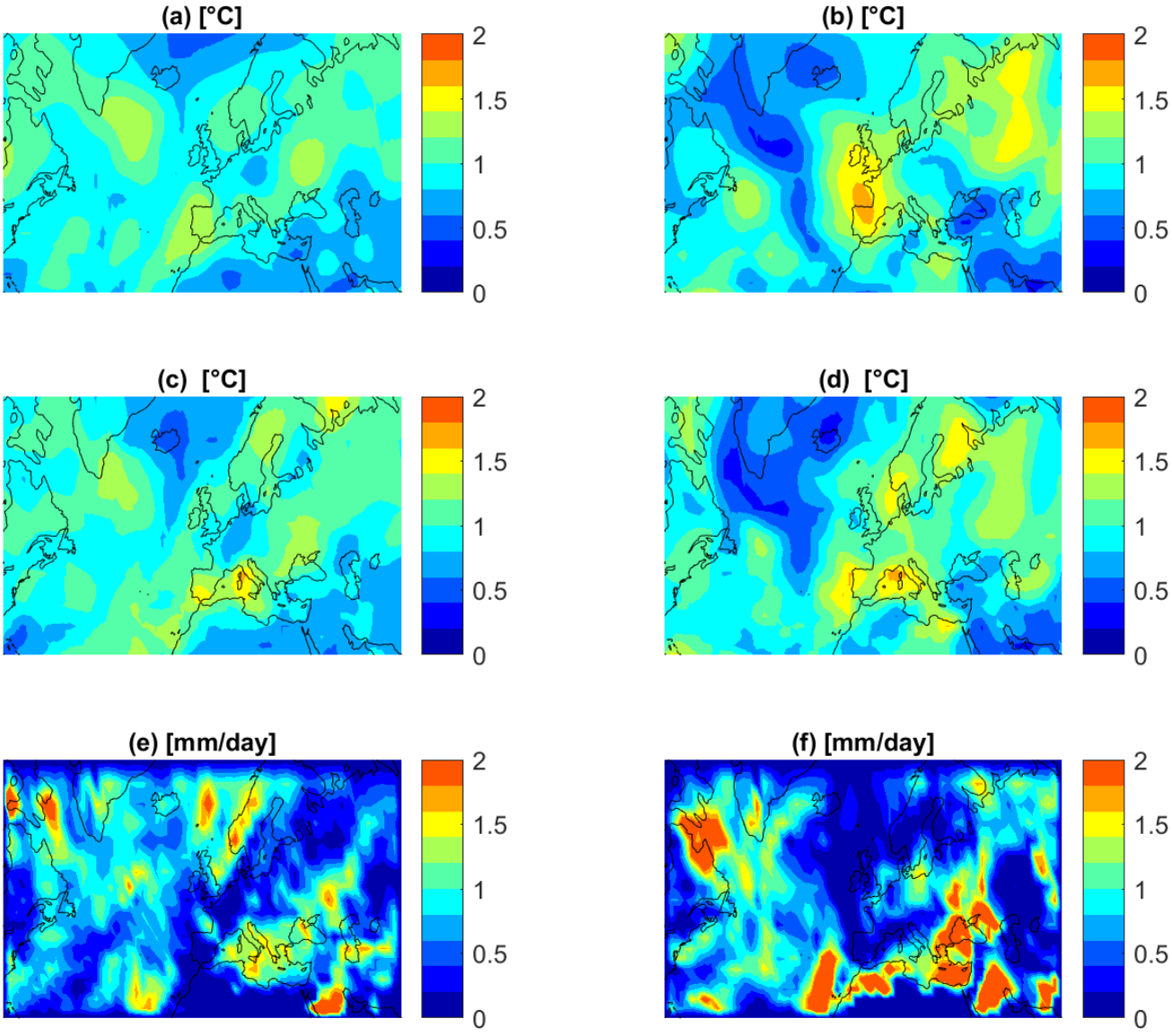

Figure 5. **Cluster uncertainty** Standard deviation of Temperature at 850 hPa [°C] (a,b), two meters temperatures [°C] (c,d), precipitation rate [mm/day] (e,f) of the two clusters of cold spells in Italy found via k-means.

3 Climate Change of Atmospheric Circulations associated to Cold Spells in PlaSiM

3.1 Model Description

175 In order to understand how the frequency of cold spell events may change in a warmer climate, we simulate different emission scenarios using PlaSim (Fraedrich et al., 2005a, b), an intermediate complexity climate model developed at the Univer-

sity of Hamburg and released open source (see https://www.mi.uni-hamburg.de/en/arbeitsgruppen/theoretische-meteorologie/modelle/plasim.html). PlaSim has been applied to a variety of problems including climate response theory (Lucarini et al., 2014), storm tracks (Fraedrich et al., 2005b), climatic tipping points (Boschi et al., 2013; Lucarini et al., 2010a), the analysis of global energy and entropy budget (Fraedrich and Lunkeit, 2008; Lucarini et al., 2010b), the simulation of extreme European heatwaves (Ragone et al., 2018), and the investigation of the late Permian climate (Roscher et al., 2011). The reason of using PlaSim with respect to higher complexity GCMs is the ability to generate long stationary simulations for which we compute reliable analogues. The horizontal resolution used in this study is about 300 km (T42, $\sim 2.8\ ^\circ \times 2.8\ ^\circ$) with ten vertical, non-equidistant levels. The dynamical core for the atmosphere is adopted from Portable University Model of the Atmosphere (PUMA). The model includes a full set of parameterizations of physical processes such as those relevant for describing radiative transfer, clouds formation, and turbulent transport across the boundary layer. The horizontal heat transport in the ocean can be prescribed or parameterized by horizontal diffusion. The ~~parametrization~~ parameterization by horizontal diffusion ~~has~~ includes a simplified representation of the large scale oceanic heat transport and then it ameliorates the realism of the resulting climate. The atmospheric dynamical processes are modelled using the primitive equations formulated for vorticity, divergence, temperature, and the logarithm of surface pressure. The governing equations are solved using a spectral transform method. In the vertical dimension, five non-equally spaced sigma (pressure divided by surface pressure) levels are used. The model is forced by diurnal and annual cycles.

3.2 Experimental set up: the simulation ensemble

In this study we consider ~~three~~ four simulations performed with T42 resolution at daily frequency, 450 years long, with a mixed layer ocean. To get reasonable response and present-day climate, one needs to add an oceanic heat transport in the mixed layer model (slab ocean, without motion). This can be done in several ways: for our set up, we tuned horizontal diffusion ($h_{\rm diff}$) to have a reasonable global mean SST and a realistic response of SST and ice to the forcing ($h_{\rm diff} = 4 \cdot 10^4$).

The first simulation is the control run (~~denoted~~ hereinafter CTRL) with radiative forcing levels representative of the recent ~~climate:~~ past climate: equivalent CO_2 concentration, including the net effect of all anthropogenic gases, is set to a value of 360 ppmv~~, corresponding to the CO_2 concentration in the year 2000.~~. Three more simulation runs were produced, based on three of the Representative Concentration Pathways (RCPs) developed for the climate modeling community as a basis for long-term and near-term modeling experiments (Van Vuuren et al., 2011a). We consider the RCP-2.6, RCP-4.5 and RCP-8.5 scenarios ~~(Riahi et al., 2011)~~(Van Vuuren et al., 2011b), which consist of ~~increasing CO_2 concentration~~ incrementing the radiative forcing from 2005 to 2100, to reach a ~~radiative forcing~~ increase of, respectively, 2.6, 4.5 and 8.5 W/m^2 compared to pre-industrial conditions. In our simulations (denoted ~~RCP26, RCP45 and RCP85~~RCP2.6, RCP4.5 and RCP8.5), the equivalent CO_2 concentration is set at the beginning to be, respectively, 490 ppm, 660 ppm and to 1470 ppm, and kept constant afterwards. These correspond to the end-of-century ~~CO2~~ equivalent CO_2 concentrations of the respective RCPs. By using these three different forcing scenarios, we are able to explore climates ranging from moderate warming to ~~non-climate~~ no climate policy.

This way, we explore three scenarios where excess heat is stored in the the atmosphere in different amounts, and we investigate which differences in the dynamics associated to cold and snowy spells in the present climate appear, if any. We will

analyse the Z500, PSL, T850 and T2M fields corresponding to the PlaSim events analogues to the cold spells clusters to characterize their dynamical and thermodynamical fingerprints, in analogy to the discussion presented in Section 2.2. Moreover, we will consider daily precipitation to check whether similar dynamics are still associated, under different RCPs, to precipitation patterns similar to the ones found in present climate.

3.2.1 Bias correction

Climate models, even those with higher complexity than PlaSim, are characterized by a finite resolution, thus leaving smaller scales unresolved, and contain several physical and mathematical simplifications that make climate simulations computationally feasible, while also introducing a certain level of approximation. This results in statistical biases that can be easily observed when comparing control runs to observations or reanalysis datasets. In order to mitigate the effects of these biases, a bias correction step can be performed. Bias correction usually consists of adjusting specific statistical properties of the simulated climate variables to a validated reference dataset in the historical period. The target statistics can be very simple, such as a central tendency index like the mean (Shrestha et al., 2017), or it may include dynamical features, such as a certain number of autocorrelation function lag or spectral density frequencies for time series data (Nguyen et al., 2016). It can aim at correcting the entire probability distribution of the observable. The correction can also be carried out in the frequency domain, so that the entire time dependence structure is preserved. For an overview of various BC methodologies applied to climate models see, for example, Teutschbein and Seibert (2012, 2013); Maraun (2016).

Given the lower complexity and the relatively coarse grid of PlaSim compared to other regional or global circulation models, we rely on simple methodologies. We apply BC only to the T850, T2M and PRP, since we will use their composites to characterize the phenomena associated to the dynamic analogues of the two clusters. No BC is usually performed on Z500 and SLP; moreover, the analogue search is based on standardized anomalies, making BC unnecessary for these variables.

For the variables characterized by ~~anomalies with~~ approximately symmetric distributions (~~Z500, SLP,~~ T850 and T2M), we adopt a simple linear scaling bias correction (Shrestha et al., 2017), which consists of constraining the CTRL mean and standard deviation of each variable to match the NCEP values, and applying the same transformation to the and RCP simulations.

For PRP, we must rely on a different method, given the strong asymmetry characterizing the distribution of precipitation. We choose quantile mapping based on regularly spaced quantiles, with a wet day correction to obtain an equal fraction of days with precipitation in the reference and corrected data: the empirical probability of nonzero precipitation is found, and the corresponding modelled value is selected as a threshold. All modelled values below this threshold are set to zero. This technique is described by Gudmundsson et al. (2012) and implemented in the `fitQmapQUANT` function from the `R` package `qmap`.

3.3 Analogues detection

We base our analysis of cold spells in PlaSim on the search of dynamic analogues (Yiou et al., 2013) in a similar way as in Faranda et al. (2020). This way of defining analogues by embedding the extreme events of interest in the climate simulation is rooted in the link between dynamical systems and extreme value theory (Lucarini et al., 2012), and the events selected as

analogues are linked to quantities such as the local attractor dimension and the persistent of the dynamical system state (Pons et al., 2020). Here we briefly sketch the methodology, redirecting the reader to the aforementioned papers.

~~Since we focus on coldspells affecting Italy, we consider the smaller domain 22.5–70N, 10W–70E, which includes Europe and Western Russia, but not the North Atlantic and North America.~~

Let X_t denote the value of a gridded variable of interest (here, the Z500 anomaly field) at time $t = 1, \ldots, T$. Let ζ represent the same variable in correspondence of one event of interest, in our case one of the Z500 anomaly fields associated to the two clusters obtained as described in Section 2.2 and shown in Figure 2c,d). We compute the metric

$$g_t = -\ln\{dist(X_t, \zeta)\},$$

where $dist(,)$ denotes a distance function, in our case the Euclidean distance. The choice of the Euclidean distance has been motivated in Yiou et al. (2013) and in Faranda et al. (2017) for the computation of dynamical indicators such as the local attractor dimension. Furthermore, the minus sign allows to interpret the g_t function as an indicator of proximity of analogues.

Let now g_c be a high percentile of the distribution of g, for example corresponding to the probability $P(g_t \geq g_c) = 0.98$: the events satisfying this condition are considered analogues of ζ. As already mentioned, we limit our analysis to the extended winter season DJFM, as these months include all the 32 selected cold spell events.

The procedure is carried out, for each cluster, according to the following steps:

1. define ζ as the Z500 anomaly field corresponding to the chosen cluster, and X_t as the ensemble of all the NCEP Z500 anomaly fields;
2. compute the metric $g^{Z500}_{t,NCEP}$ using data selected at step 1;
3. determine the critical value g_c^{Z500} such that $P(g^{Z500}_{t,NCEP} \leq g_c^{Z500}) = p_1$;
4. now take PlaSim Z500 fields as X_t, while keeping the same reference field ζ;
5. compute the metrics $g^{Z500}_{t,r}$ using Z500 from PlaSim runs, with $r =$ CTRL, ~~RCP26, RCP45, RCP85~~RCP2.6, RCP4.5, RCP8.5;
6. estimate probabilities $\pi_{1,r} = P(g^{Z500}_{t,r} \leq g_c^{Z500})$ and compare them to the reference value p_1;
7. consider cold spell analogues all events satisfying $P(g^{Z500}_{t,r} \geq g_c^{Z500}) = p_1$;

Steps 1 – 3 select the (1-p_1) fraction of closest winter analogues of the two main configurations leading to the selected cold spells. Steps 4 – 6 allow to determine whether the frequency of the configuration is significantly different in the PlaSim scenarios compared to NCEP, and in which direction. This way, we can establish if climate change can affect atmospheric dynamics, leading to an atmosphere more or less conducive for synoptic configurations that can result in a cold spell. In step 7 we then select the analogues of the configurations of interest in the PlaSim runs. This way, we can study the composites of other variables of interest, namely temperature and precipitation, to assess the phenomena associated the same dynamics under different climate scenarios. In our analysis, we choose $p_1 = 0.98$, so that we consider as analogues the 2% NCEP Z500 anomaly fields closest to the cluster fields.

3.4 Results

Our first result follows from the estimation of the probabilities described at step 6. in the previous paragraph. These are the probabilities ~~$\pi_{1,r}$~~ $\pi_{i,r}$ that the Z500 field at date t from run r is an analogue of the ~~event of interest~~ centroid of cluster $i = 1, 2$ as close as the $(1 - p_1)\%$ of the closest NCEP Z500 fields. In particular, we are interested in the differences ~~$\Delta p_{1,r} = (\pi_{1,r} - p_1)$. If $\Delta p_{1,r} > 0$, the reference event~~ $\Delta p_{i,r} = (\pi_{i,r} - p_1)$. If $\Delta p_{i,r} > 0$, the configuration is more extreme and less frequent than in historical climate. On the contrary, values ~~$\Delta p_{1,r} < 0$~~ $\Delta p_{i,r} < 0$ indicate a more recurring event. The percentage change in frequency of events that are cold spell dynamic analogues can be obtained as ~~$-\Delta p_{1,r}/(1 - p_1)$~~ $-\Delta p_{i,r}/(1 - p_1)$.

The results of this analysis are summarized in Table 1.

	Cluster 1		Cluster 2	
run	$\pi_{1,r}$	$-\Delta p_{1,r}/(1-p_1)$	~~$\pi_{1,r}$~~ $\pi_{2,r}$	~~$-\Delta p_{1,r}/(1-p_1)$~~ $-\Delta$
CTRL	~~0.9797~~ 0.9683	+~~1.35~~58.6%	~~0.969~~ 0.9556	+~~53.4~~122.1
~~RCP26~~ RCP2.6	~~0.978 (0.977~~0.973475 (0.9617)	+~~12.5~~32.6% (+~~13.8~~91.3%)	~~0.977 (0.966~~0.9711472 (0.9467)	+~~14.4~~44.3% (+~~67.~~
~~RCP45~~ RCP4.5	~~0.976 (0.976~~0.9726 (0.9609)	+~~20.1~~37.0% (+~~21.4~~95.7%)	~~0.975 (0.964~~0.9642 (0.9397)	+~~27.0~~79.2% (+~~80.~~
~~RCP85~~ RCP8.5	~~0.967 (0.967~~0.9575 (0.9458)	+~~62.9~~112.5% (+~~64.2~~171.2%)	~~0.967 (0.956~~0.9334 (0.9090)	+~~67.5~~232.9% (+~~71~~

Table 1. Change in frequency of cold spell analogues for each of the considered events, divided by cluster. The values corresponding to the RCPs are adjusted by subtracting the values relative to the CTRL run, which quantify PlaSim's bias in analogues frequency; unadjusted values are shown in parentheses.

The results for the CTRL run inform us about the capability of PlaSim to reproduce the frequency of the two dynamical fingerprints of cold spells associated to the two clusters of events. ~~While the Atlantic ridge configuration has a similar frequency (+1.35%) the Scandinavian blocking appears to be sensibly more frequent (+53.4%)~~ Both configurations are much more frequent in PlaSim than in ~~the reanalysis.~~ NCEPv2, with a +58.6% frequency of the circulation associated to the cluster 1 centroid, and +122.1% for cluster 2. We offset the results for the RCP scenarios by subtracting these frequency biases; ~~raw~~ unadjusted results are shown in parentheses.

Both configurations become increasingly more frequent with growing ~~CO2 concentration~~radiative forcing. It is worth mentioning that this analysis does not discriminate between an increased number of Atlantic ridge and Scandinavian blocking episodes and their longer persistence, both of which may lead to more analogues. Nevertheless, these result clearly suggests a higher number of days characterized by configurations leading to a flow of Arctic air towards the Mediterranean area under climate change.

Figure 6 shows the composites of Z500 analogues fields in the CTRL (a,b) and RCP (c-h) runs for analogues of cluster 1 (a,c,e,g) and cluster 2 (b,d,f,h). ~~Figure ?? shows the corresponding standardized anomaly fields~~The isolines show the corresponding positive (in red) and negative (in black) standardized anomalies, on which we base the analogue search. The Z500 fields are associated with the SLP fields shown in Figure 7. Whereas the anomaly patterns ~~observed for the CTRL run strongly~~ overall resemble those of the NCEP reanalysis for both Z500 and SLP, we observe that, when increasing the ~~CO2~~ equivalent CO_2 concentration, the ~~analogues tend to be associated with cut offs in the full Z500 field: isolated patches of low potential vorticity disconnected by the main polar vortex that shifts further to the North. The Z500 fields are associated with the SLP fields shown in Figure 7. For the control (a, b) and the RCP 2.6 (c,d) simulations, a cyclogenesis on the Ionian see is clearly visible. In the RCP4~~magnitude of the negative anomalies in the Mediterranean area decreases, especially in RCP8.5~~(e,f) and RCP 8.5 (g,h) this cyclonegesis is almost absent~~.

Figure 8 show the composites of the T850 fields. As expected, with growing ~~CO2 concentration~~radiative forcing, negative temperatures are confined progressively more to the North and East, with only an isolated cold patch still persisting over Russia under ~~RCP85~~RCP8.5. A similar behaviour is also observed for T2M, shown in ~~Figure~~ figure 9. Indeed, under stronger warming scenarios, these configurations seem to be associated to winter heat waves over Central-Northern Europe, with higher temperatures compared to the Mediterranean area. We remark that, in the ~~RCP 2.6~~ RCP2.6 simulation, T850 and T2M values are still low enough to be associated with snow precipitation in most of the hills and mountain areas of Italy.

The precipitation patterns associated to these analogues are shown in Figure 10. The distribution of precipitation in the CTRL run is fairly similar to those of NCEP ~~and not much different between the two~~ cluster 2 for both clusters, showing the most abundant precipitation over the Central-Eastern Mediterranean Sea including most of Italy, ~~over~~ the Balkans, Greece, Turkey and the Black Sea; ~~precipitation patches are also observed over France, the Iberian peninsula and the UK, and over Eastern Europe. Overall, a decrease in precipitation associated to these patterns can be observed with growing CO2 concentrations over the Western Mediterranean and France in particular, while the area between the Central Mediterranean - including Italy - and the Black Sea is interested by the most intense precipitations under all scenarios.~~ a lack of precipitation is observed on Southern Italy and Sardinia for analogues of cluster 1.

In summary, in ~~the warmer RCP climates~~a warmer climate, the frequency of dynamic configurations leading to Z500 fields similar to the geopotential maps in Fig. 2 may increase even dramatically, depending on the scenario. Clearly, this does not imply that Italy would paradoxically experience increasing snowfalls in the RCP climates. Indeed, the PlaSim simulations display a clear increase of temperature, that would make snowfall overall much less likely, at least at low altitudes.

Figures 11-15 show the root mean squared deviation (RMSD) of the analogues of each cluster from the corresponding cluster centroid. Compared to the within-cluster standard deviations shown in figures 4-5, higher uncertainty is associated to the position of the high- and low-level cyclones and anticyclones among the analogues, particularly for the SLP minimum in cluster 1. Moreover, very high uncertainty is associated with the negative anomalies of both T850 and T2M, suggesting that the composites in figures 8-9 encompass configurations leading to very different thermodynamic set-ups. similar or slightly lower uncertainty than in NCEP is, instead, associated to the area characterized by precipitations on the Mediterranean area.

~~**500 hPa Geopotential heights in PlaSIM simulations:** Average of the 500 hPa geopotential height mfor Cluster 1 (a,c,e,g), Cluster 2 (b,d,f,h) of analogues. (a,b) control run, (c,d) RCP 2.6 run, (e,f) RCP 4.5 run, (g,h) RCP 8.5 run~~

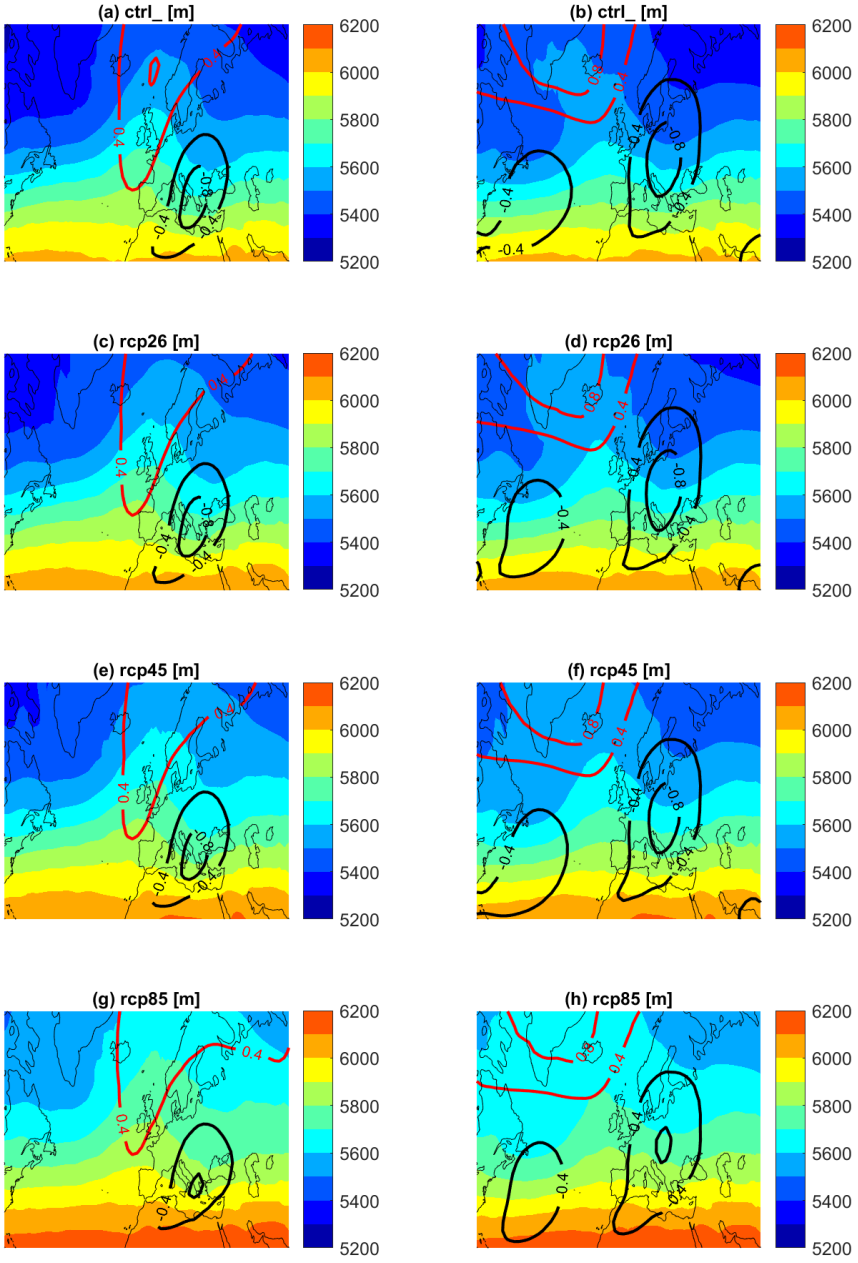

Figure 6. 500 hPa Geopotential heights in PlaSIM simulations: Average of the 500 hPa geopotential height [m] for Cluster 1 (a,c,e,g), Cluster 2 (b,d,f,h) of analogues. (a,b) control run, (c,d) RCP2.6 run, (e,f) RCP4.5 run, (g,h) RCP8.5 run. Isolines represent positive (in red) and negative (in black) standardized anomalies.

~~500 hPa Geopotential heights standardized anomalies in PlaSIM simulations:~~ ~~Average of the 500 hPa geopotential height standardized anomalies for Cluster 1 (a,c,e,g), Cluster 2 (b,d,f,h) of analogues. (a,b) control run, (c,d) RCP 2.6 run, (e,f) RCP 4.5 run, (g,h) RCP 8.5 run~~

~~Sea level pressure in PlaSIM simulations:~~ ~~Average of the sea-level pressure hPafor Cluster 1 (a,c,e,g), Cluster 2 (b,d,f,h) of analogues. (a,b) control run, (c,d) RCP 2.6 run, (e,f) RCP 4.5 run, (g,h) RCP 8.5 run~~

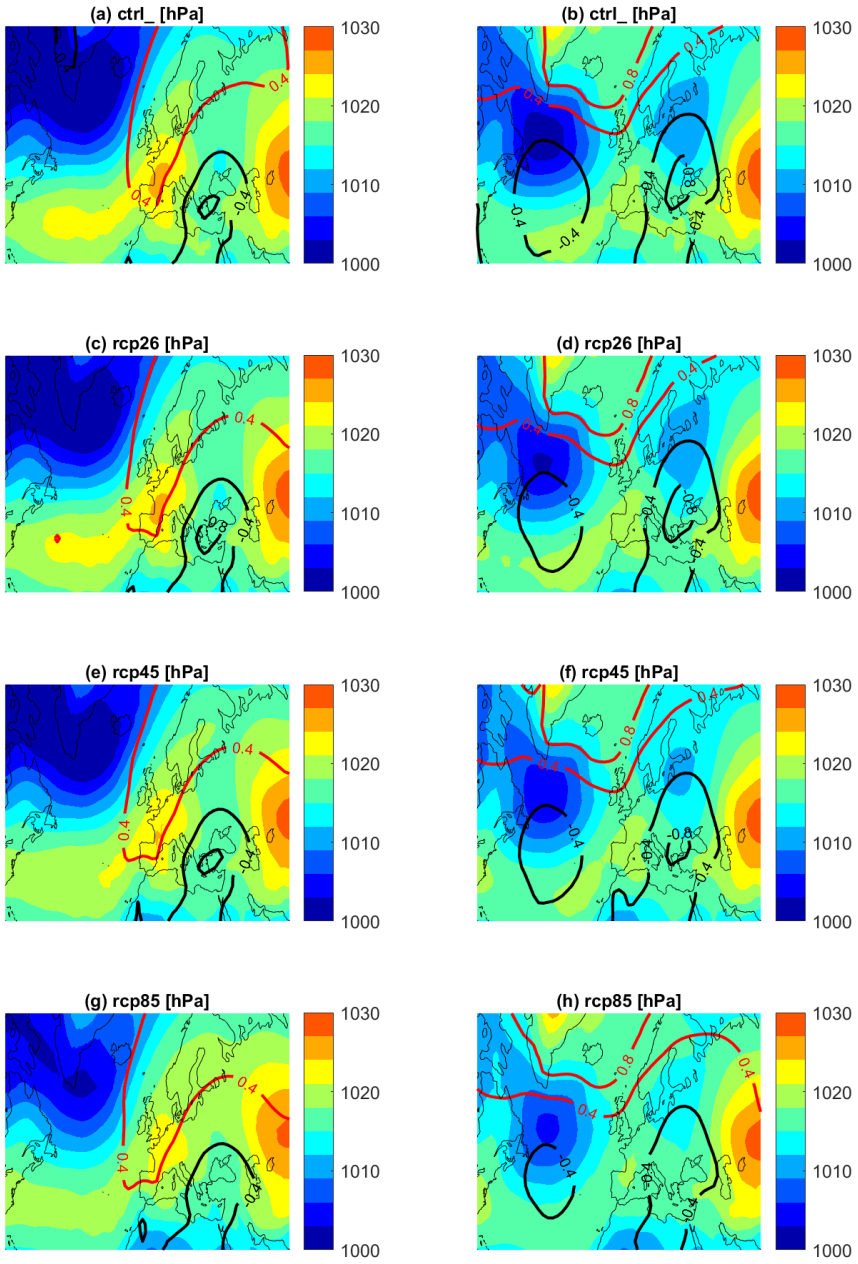

~~**850 hPa Temperature in PlaSIM simulations:** Average of the 850 hPa temperature °Cfor Cluster 1 (a,c,e,g), Cluster 2 (b,d,f,h) of analogues. (a,b) control run, (c,d) RCP 2.6 run, (e,f) RCP 4.5 run, (g,h) RCP 8.5 run~~

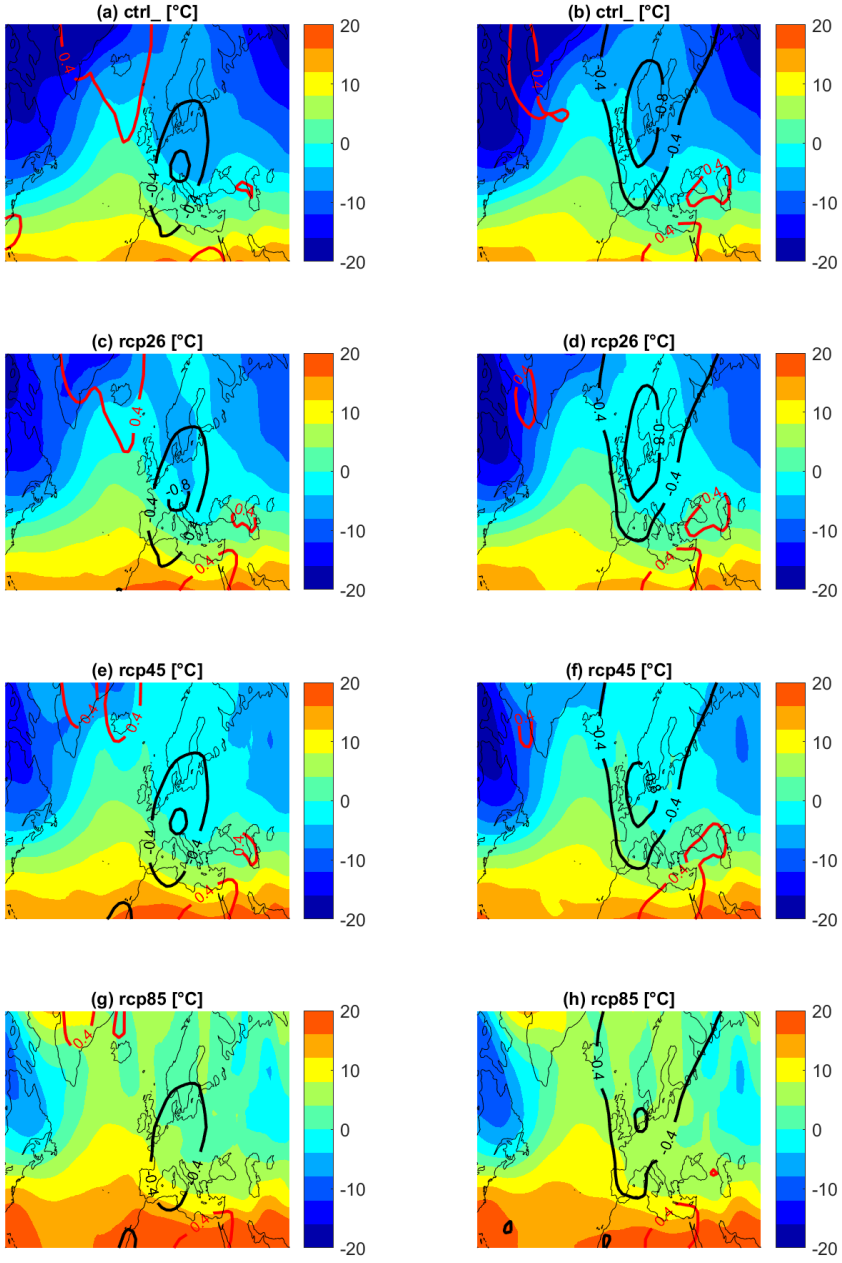

Figure 8. **850 hPa Temperature in PlaSIM simulations:** Average of the 850 hPa temperature [°C] for Cluster 1 (a,c,e,g), Cluster 2 (b,d,f,h) of analogues. (a,b) control run, (c,d) RCP2.6 run, (e,f) RCP4.5 run, (g,h) RCP8.5 run. Isolines represent positive (in red) and negative (in black) standardized anomalies.

~~**Two meters temperatures in PlaSIM simulations:** Average of the two meters temperature °Cfor Cluster 1 (a,c,e,g), Cluster 2 (b,d,f,h) of analogues. (a,b) control run, (c,d) RCP 2.6 run, (e,f) RCP 4.5 run, (g,h) RCP 8.5 run~~

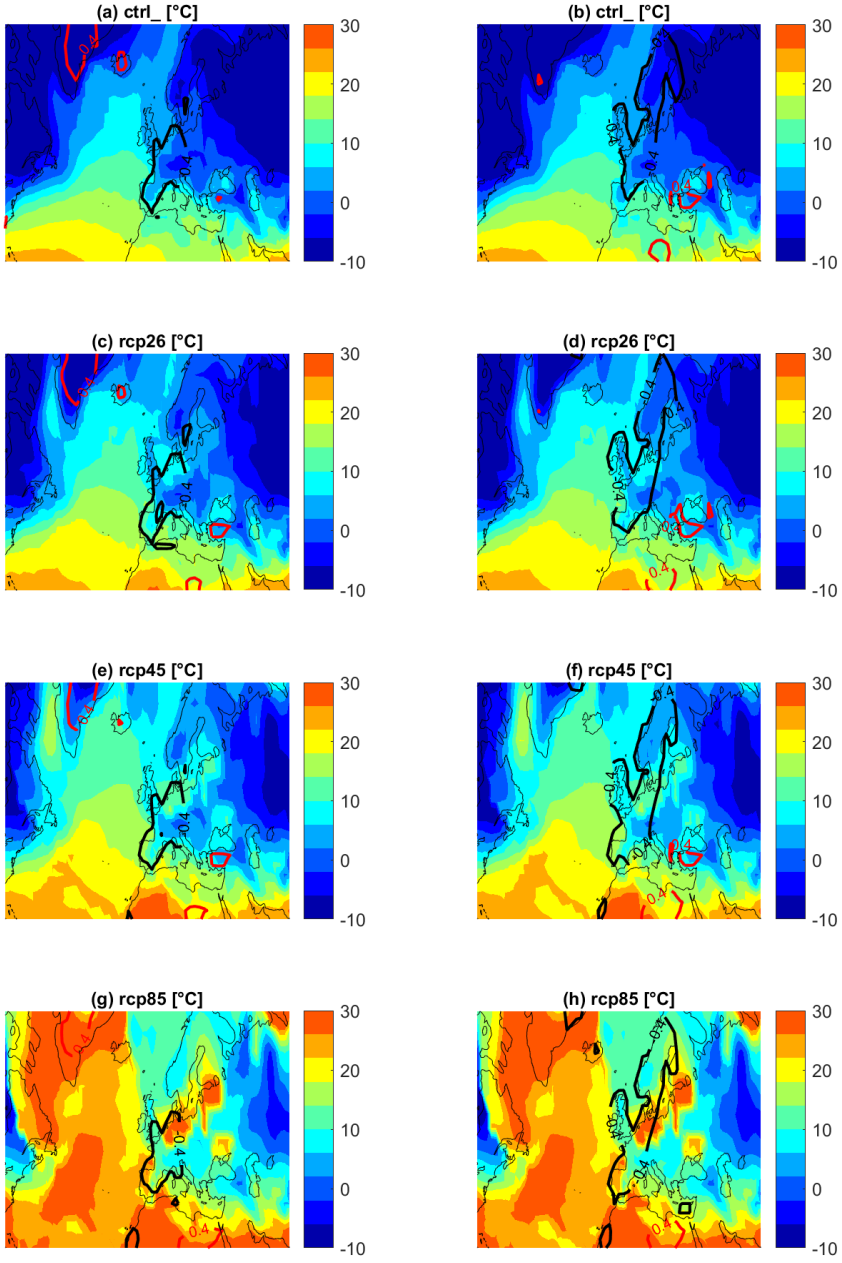

Figure 9. **Two meters temperatures in PlaSIM simulations:** Average of the two meters temperature [°C] for Cluster 1 (a,c,e,g), Cluster 2 (b,d,f,h) of analogues. (a,b) control run, (c,d) RCP2.6 run, (e,f) RCP4.5 run, (g,h) RCP8.5 run. Isolines represent positive (in red) and negative (in black) standardized anomalies.

~~**Daily precipitation rates in PlaSIM simulations:** Average of the daily precipitation rates mm/dayfor Cluster 1 (a,c,e,g), Cluster 2 (b,d,f,h) of analogues. (a,b) control run, (c,d) RCP 2.6 run, (e,f) RCP 4.5 run, (g,h) RCP 8.5 run~~

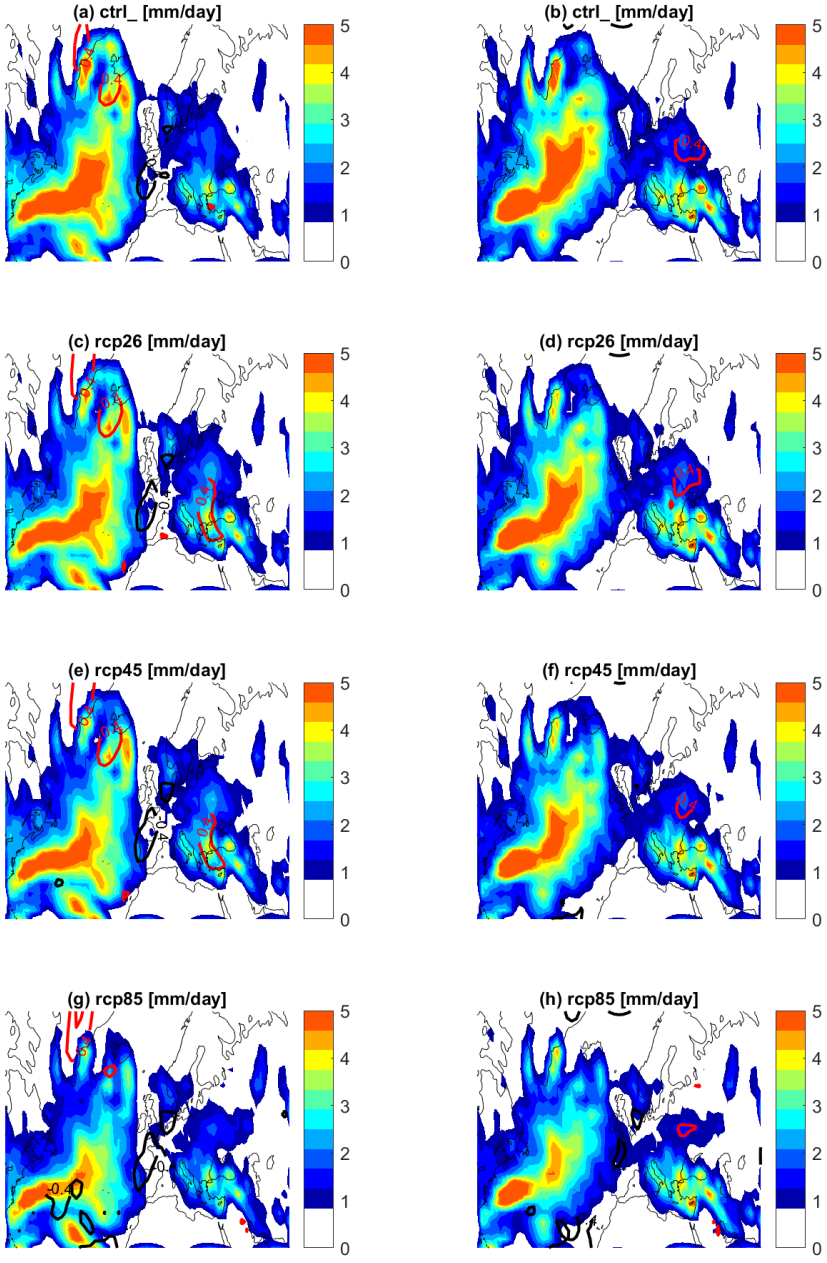

Figure 10. **Daily precipitation rates in PlaSIM simulations:** Average of the daily precipitation rates [mm/day] for Cluster 1 (a,c,e,g), Cluster 2 (b,d,f,h) of analogues. (a,b) control run, (c,d) RCP2.6 run, (e,f) RCP4.5 run, (g,h) RCP8.5 run. Isolines represent positive (in red) and negative (in black) standardized anomalies.

4 CMIP5 analysis

Given the PlaSim limitations in resolution and capabilities of representing weather patterns associated with extreme events, we analyse whether patterns associated to cold-spells over Italy become more frequent also in CMIP5 models using the methodolgy outlined in Faranda et al. (2020). We extract the daily Z500 fields corresponding to the 32 cold spell events. We then embed these observed events into historical simulations (1951–2000) , and projections (2051–2100) under a medium (RCP4.5) and high (RCP 8.5) emissions scenarios (Van Vuuren et al., 2014) of the CMIP5 models (Taylor et al., 2012) given in Table **??**. In the extreme event attribution vocabulary, we consider the historical simulations (1951-2000) as the factual world, i. e. the actual world with the current level of anthropogenic emission. The two RCP scenarios correspond to counterfactual worlds. Given that the models have biased representation of the geopotential heights, we apply a statistical bias correction (Michelangeli et al., 2009; Panofsky — allowing to account for climate change (Vrac et al., 2012) — on the Z500 fields, before the analysis. We perform two types of bias correction: one by preserving the spatial average trend in z500, and one by removing those trend. The removed Z500 spatial average trend corresponds to the spatially uniform, seasonal shift of Z500, mainly caused by the warming over the region. Hence, by removing it, we also removed the first order thermodynamic effect of warming on Z500 fields. Therefore, the resulting anomalies —- which are further bias corrected —-, once embedded into our analogs-based methodology, indicate changes mostly due to dynamical changes of the state of the atmosphere. All coldspells (Figure **??**) will yield better analogs in RCP4.5 and RCP 8.5 than in the historical periods (i.e., negative change in the average Euclidean distance), more slightly for RCP8.5. This decreases in the analogs distance imply that circulation patterns associated with these cold spells become more frequent in warmer climates, as represented by CMIP5 models. The decrease is of relative magnitude 0.1 for RCP 4.5 and 0.15 for RCP 8.5 when the spatial trend is preserved and of order 0.05 for RCP4.5 and 0.07 for RCP 8.5 when the trend is removed. These results suggest that thermodynamics contribute for half of the magnitude of analogues increase. The results obtained here for CMIP5 are consistent with the findings obtained with PlaSim for RCP 8.5 scenarios. Note that, contrarily to what we find here for cold-spells over Italy, the results obtained in Faranda et al. (2020) for four cold-spells events over Europe, found a substantial decrease in the frequency of future analogues. This suggests that the results obtained here are specific for the Italian case and cannot be generalized to cold spells over other areas of Europe, consistently with what found by Faranda (2020).

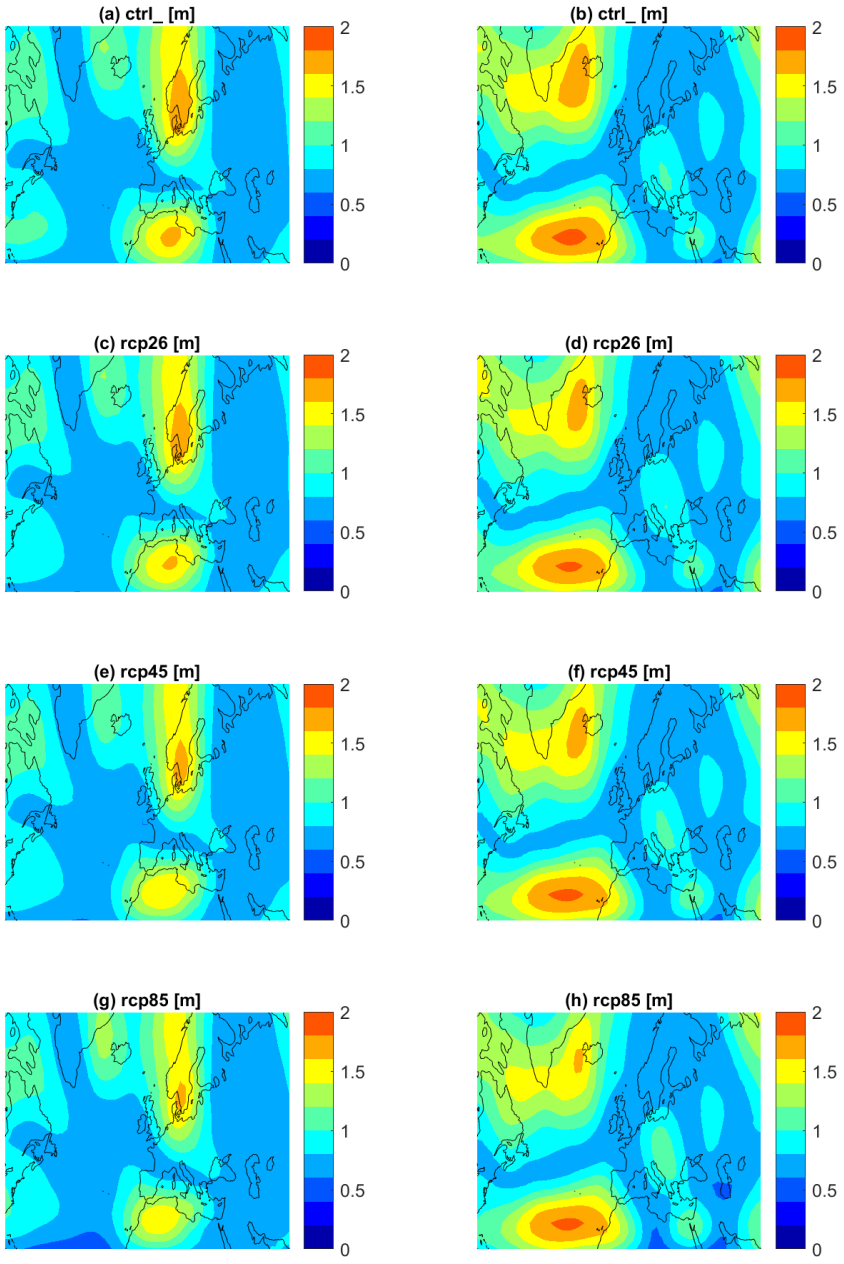

Figure 11. 500 hPa Geopotential heighte uncertainty in PlaSIM analogues: Root mean squared difference in 500 hPa geopotential height [m] between analogues and cluster centroids for Cluster 1 (a,c,e,g), Cluster 2 (b,d,f,h). (a,b) control run, (c,d) RCP2.6 run, (e,f) RCP4.5 run, (g,h) RCP8.5 run

~~**Analogues in CMIP5 simulations** Relative changhes in average analogues distance for RCP4.5 and RCP8.5 simulations. Each dots represent the median over all cold-spell events in the model givn with the color-code in the legend. Black horizontal line~~

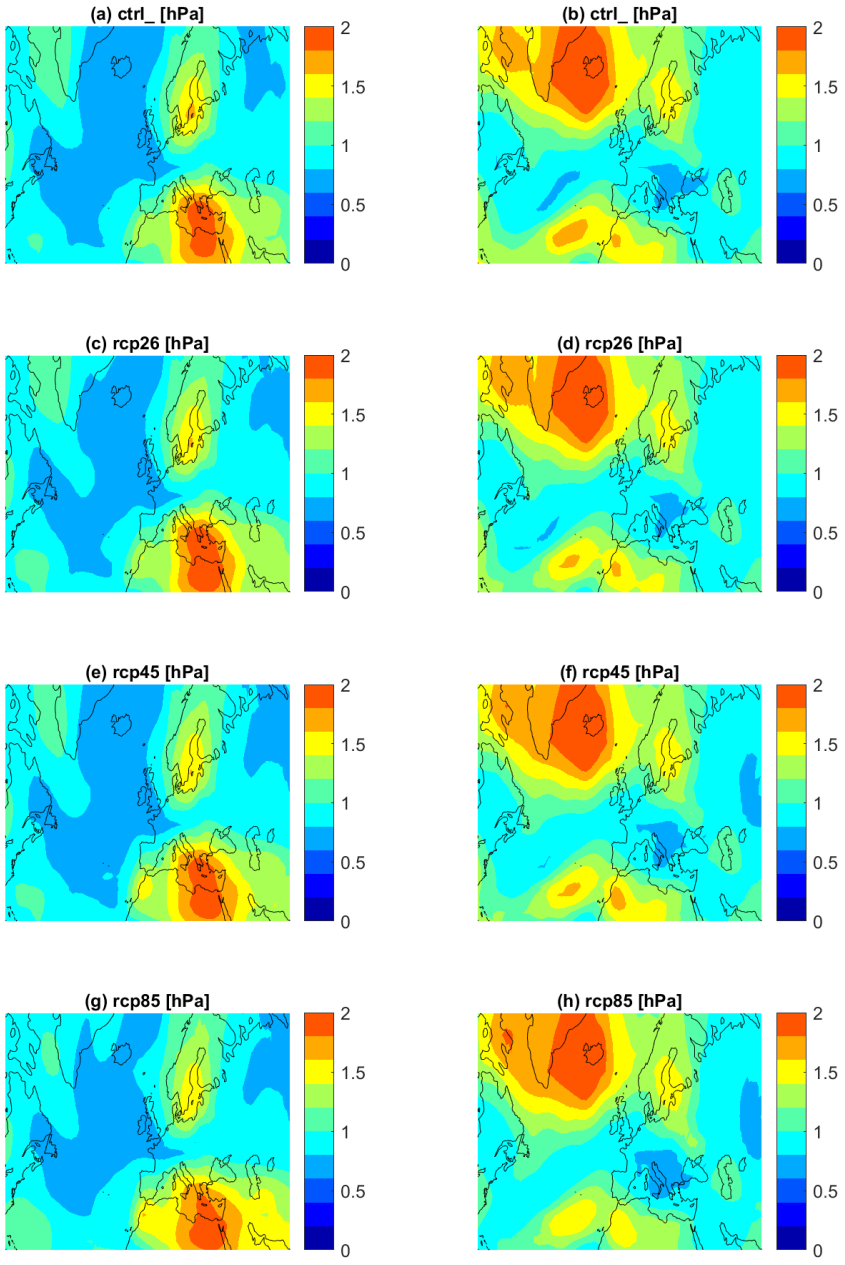

~~is the multimodel mean.~~

Figure 12. **Sea level pressure uncertainty in PlaSIM analogues.** Root mean squared difference in sea level pressure [hPa] between analogues and cluster centroids for Cluster 1 (a,c,e,g), Cluster 2 (b,d,f,h). (a,b) control run, (c,d) RCP2.6 run, (e,f) RCP4.5 run, (g,h) RCP8.5 run

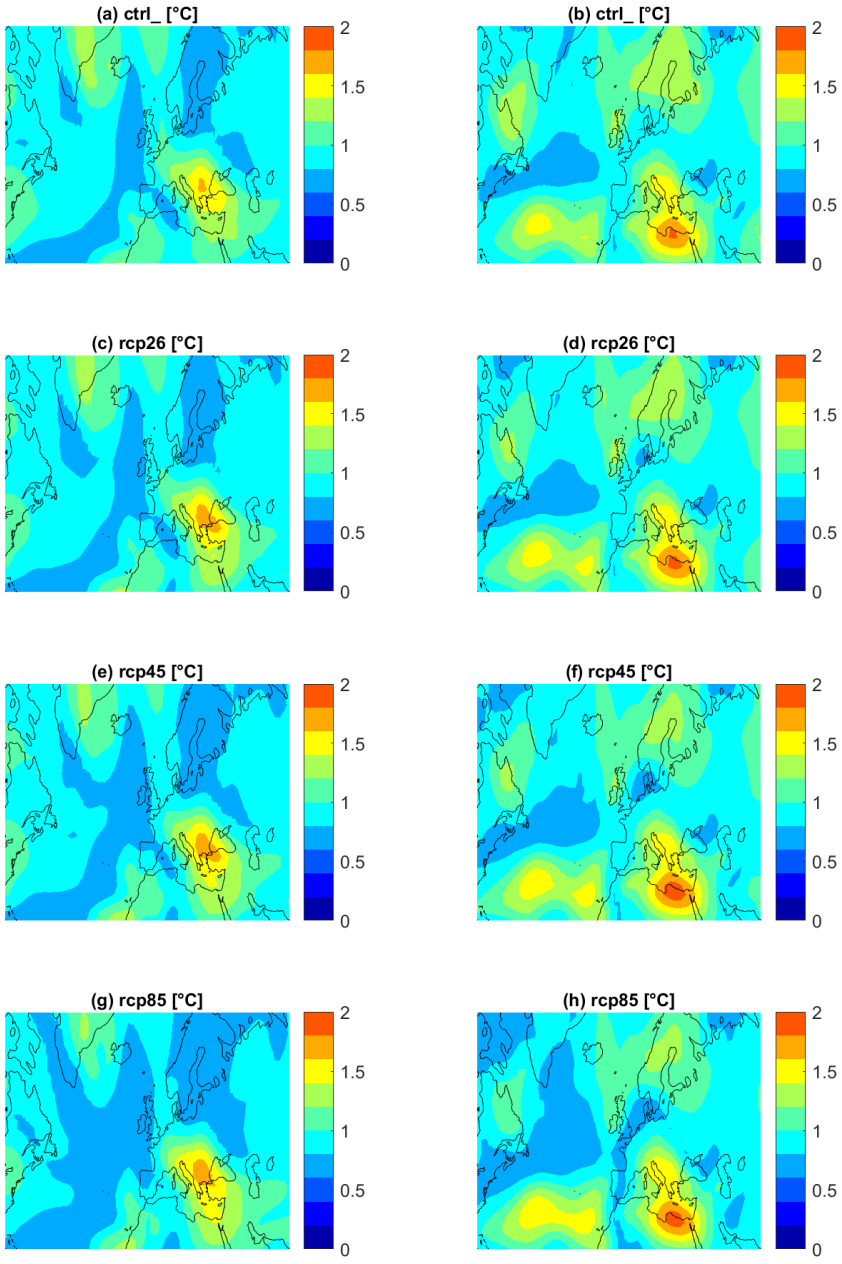

Figure 13. **850 hPa Temperature uncertainty in PlaSIM analogues:** Root mean squared difference in 850 hPa Temperature [°C] between analogues and cluster centroids for Cluster 1 (a,c,e,g), Cluster 2 (b,d,f,h). (a,b) control run, (c,d) RCP2.6 run, (e,f) RCP4.5 run, (g,h) RCP8.5 run

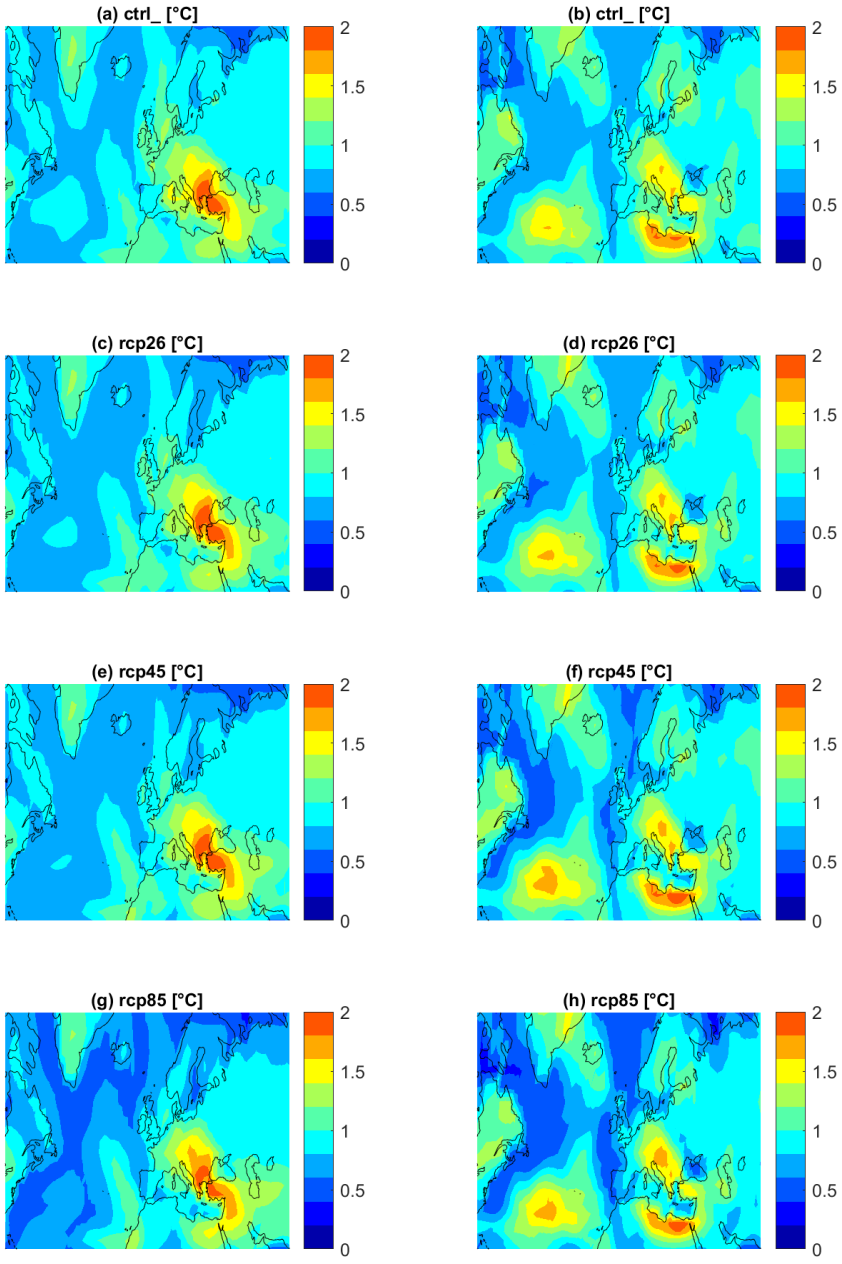

Figure 14. **Two meters Temperature uncertainty in PlaSIM analogues:** Root mean squared difference in two meters Temperature [°C] between analogues and cluster centroids for Cluster 1 (a,c,e,g), Cluster 2 (b,d,f,h). (a,b) control run, (c,d) RCP2.6 run, (e,f) RCP4.5 run, (g,h) RCP8.5 run

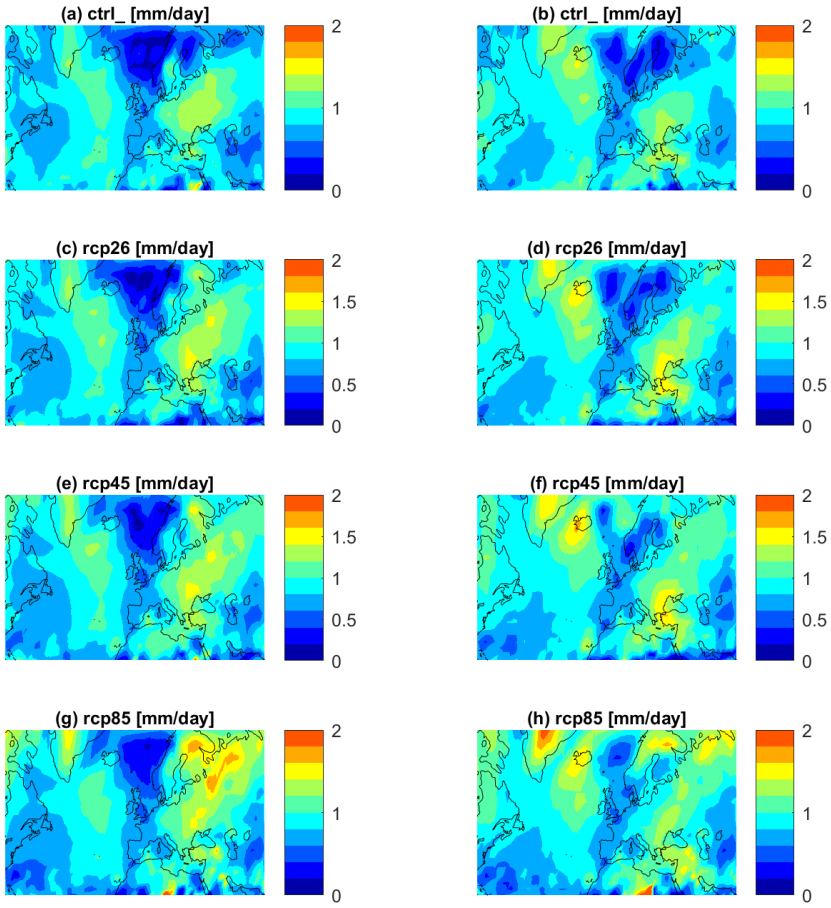

Figure 15. Daily precipitation rate uncertainty in PlaSIM analogues: Root mean squared difference in daily precipitation rates [mm/day] between analogues and cluster centroids for Cluster 1 (a,c,e,g), Cluster 2 (b,d,f,h). (a,b) control run, (c,d) RCP2.6 run, (e,f) RCP4.5 run, (g,h) RCP8.5 run

4 Discussion and conclusion

We have characterized high-impact cold spells that affected Italy in the course of the past ~~60~~ 68 years by assessing their common dynamical large scale signature. Despite the differences in duration, snowfall and temperature recorded during each event, the corresponding Z500 fields can be grouped according two main dynamic fingerprints. Both are characterized by the presence of a low pressure area over the Central Mediterranean, associated to an anticyclone either ~~elevated over Western Europe (cluster~~

1), or zonally tilted between Western Europe and Russia, with pressure maxima over Central Europe (cluster 1), or elevated over Western Europe (cluster 2). In both cases, cold air is drawn towards Italy by the Mediterranean low pressure area, flowing mainly from Scandinavia Russia (cluster 1) or Russia Scandinavia (cluster 2).

Then, after assessing the capability of PlaSim to reproduce dynamic analogues of these events in the CTRL run, we have studied the influence of climate change on the frequency of such analogues using three steady-state increased emission scenarios. The PlaSim control run showed a tendency to well represent the frequency of Atlantic ridge and to over-estimate the frequency of the Scandinavial blockingboth configurations. All three RCP runs are associated to more frequent configurations potentially leading to cold spells, with frequency increasing with CO2 equivalent CO_2 concentration, and a precipitation pattern that does not change substantially over the Mediterranean region. This increased frequency of Atlantic Ridge and Scandinavian-like blocking patterns could be associated to a wealth of phenomena driven by the mean antrhopogenic climate change but still debated in the current scientific literature such as the Arctic Amplification or the increased land-sea temperature contrast (Cohen et al., 2020; Hamouda et al., 2021). Contrary arguments show an increase in flow zonality over the North Atlantic but mostly for the Autumn (de Vries et al., 2013) and the Summer seasons (Fabiano et al., 2021).

Since temperatures are projected do be contextually higher, cold spells and snow are naturally expected to decrease overall, especially under RCP45 and RCP85RCP4.5 and RCP8.5; however, we argue that the formation of cold air over the Arctic winter would not be completely suppressed, hence making cold spell events still possible, and remain relatively likely under the mitigated RCP26 RCP2.6 scenario. This observation is particularly important, as RCP26 RCP2.6 is representative of the current target to comply with the requirements of Paris agreements Arias et al. (2021)the Paris Agreement (Arias et al., 2021).

Moreover, the temperature fields shown in Figures 6-10 are obtained averaging over a large number of events, but temperatures low enough to generate snowfall will still be possible in single events. Considering the increased likelihood of the associated dynamical configuration, this is an important message, as the disruptive effects of these events may be exacerbated by lower attention and preparedness in much warmer climates.

This study comes with some caveats and limitations: although we have validated the behavior of PlaSim against the NCEP reanalysis, results on frequency changes for cold spells crucially depend on the position and the destabilization of the jet stream. It is known that different climate models have a different response of jet stream dynamics to climate change (Arctic Amplification (Cohen et al., 2014) or Zonalization (Francis and Vavrus, 2012)).

The use of an intermediate complexity model like PlaSim allowed us to evaluate the climate change of atmospheric dynamics associated to cold spells in a steady, much warmer climate, showing how the frequency and intensity of cold spells may decrease less than expected, due to a higher likelihood of synoptic configuration favourable for cold air to flow towards the Mediterranean. However, we plan to extend our analysis to higher complexity GCM end-of-century simulations such as CMIP6, to gain a more robust understanding of the distribution and phase of precipitation during this type of event.

List of CMIP5 Models Analysed. The resolution refers to the average horizontal resolution.No. Model Institution/ID Country Reolution 01 BCC-CSM1-M Beijing Climate Center China 1.125 × 1.125 02 BCC-CSM1-1 Beijing Climate Center China 2.81 × 2.79 03 BNU-ESM Beijing Normal University Earth System Model China 2.81 × 2.81 04 CANESM2 Canadian Centre for Climate Modelling and Analysis Canada 2.81 × 2.81 05 CMCC-CMS Centro Euro-Mediterraneo sui Cambiamenti

~~Climatici Italy 1.87 × 1.87 06 CNRM-CM5 CNRM-CERFACS France 1.40 × 1.40 07 GFDL-ESM2G Geophysical Fluid Dynamics Laboratory, NOAA USA 2.5 × 2.02 08 GFDL-ESM2M Geophysical Fluid Dynamics Laboratory, NOAA USA 2.5 × 2.02 09 HadGEM2-CC MetOffice-Hadley Centre UK 1.87 × 1.25 10 IPSL-CM5A-MR Institute Pierre Simon Laplace, IPSL France 2.5 × 1.26 11 IPSL-CM5B-LR Institute Pierre Simon Laplace, IPSL France 3.75 × 1.89 12 MIROC-ESM-CHEM MIROC Japan 2.81 × 2.79 13 MPI-ESM-LR Max Planck Institute for Meteorology, MPI Germany 1.87 × 1.87 14 MPI-ESM-MR Max Planck Institute for Meteorology, MPI Germany 1.87 × 1.87 15 MRI-CGCM3 Meteorological Research Institute, MRI Japan 1.125 × 1.16 NorESM1-M Norwegian Climate Center Norway 2.5 × 1.89~~

Acknowledgements

This work was supported by the ANR-TERC grant BOREAS. We thank Fabio D'Andrea and Aglaé Jézéquel (Laboratoire de Météorologie Dynamique, Paris, France) for useful discussion on the paper. FL acknowledge support by the Deutsche Forschungsgemeinschaft (DFG,German Research Foundation) through the University Hamburg's Cluster of Excellence Integrated Climate System Analysis and Prediction (CliSAP), and under Germany's Excellence Strategy - EXC 2037 'Climate, Climatic Change, and Society' (CliCCS) - Project Number: 390683824, as contribution to the Center for Earth System Research and Sustainability (CEN) of University Hamburg's. The authors acknowledge the support of the INSU-CNRS-LEFE-MANU grant (project DINCLIC).

Author Contribution

D.F. conceived the idea of the study, and designed the methodology with C.N.; M.D. and S.T. performed the simulations in consultation with F.L. and F.P. executed the statistical analysis of the results. M.D., F.P. and D.F. performed the study, P.Y., C.N., F.L. and D.F. discussed the results and implications and commented on and edited the manuscript.

Competing interests. The authors declare no competing interest.

References

3bmeteo.com: www.3bmeteo.com, last access: 26/07/2020.

Adjoua, M.F., J. S. O. A. V. M. D. D. S. B. N. T.: A bias-corrected CMIP5 dataset for Africa using CDF-t method. A contribution to agricultural impact studies, Earth System Dynamics, 9, 313 – 338, https://doi.org/10.5194/esd-9-313-2018, 2018.

Aeronautica.Militare: www.clima.meteoam.it, last access: 26/07/2020.

Aljazeera: Winter digs in across Central and Eastern Europe., Aljazeera of 07/01/2017.

ANNALI/A1956: www.uirsicilia.it/dati/ANNALI/A1956, last access: 26/07/2020.

ansa.it: www.ansa.it, last access: 26/07/2020.

ansamed.info: www.ansamed.info, last access: 26/07/2020.

Arias, P., Bellouin, N., Coppola, E., Jones, R., Krinner, G., Marotzke, J., Naik, V., Palmer, M., Plattner, G.-K., Rogelj, J., et al.: Climate Change 2021: The Physical Science Basis. Contribution of Working Group I to the Sixth Assessment Report of the Intergovernmental Panel on Climate Change; Technical Summary, 2021.

Arpa: Piemonte.

Arpa: Puglia.

Arpa, F. V. G.: www.osmer.fvg.it, Arpa Friuli Venezia Giulia last access: 26/07/2020.

Arpa Liguria, A. I.: Arpa Liguria Annali Idrologici.

Arpa Regione Emilia Romagna, A. I.: Arpa Regione Emilia Romagna Annale Idrologico.

Arpa Sardegna, A. A. e. C. d. S.: Arpa Sardegna, Analisi Agrometeorologica e Climatologica della Sardegna.

Arpae.it: www.Arpae.it, last access: 26/07/2020.

Arpav: www.arpaveneto.it, Arpa Veneto, last access: 26/07/2020.

Asnaghi, G.: Como e il Lario sotto la neve. Macchione Ed. Varese, Peirone, F, 2014.

Ayar, P. V., Vrac, M., Bastin, S., Carreau, J., Déqué, M., and Gallardo, C.: Intercomparison of statistical and dynamical downscaling models under the EURO-and MED-CORDEX initiative framework: present climate evaluations, Climate dynamics, 46, 1301–1329, 2016.

Bailey, K. D.: Method of Social Research, The Free Press, New York., 1994.

Barnes, E. A., Dunn-Sigouin, E., Masato, G., and Woollings, T.: Exploring recent trends in Northern Hemisphere blocking, Geophysical Research Letters, 41, 638–644, 2014.

Basilicata, Protezione Civile, A. I.: Agenzia Regionale Protezione Civile Basilicata Annali Idrologici.

Bolzano, P. C.: Protezione Civile Provincia Autonoma di Bolzano.

Boschi, R., Lucarini, V., and Pascale, S.: Bistability of the climate around the habitable zone: A thermodynamic investigation, Icarus, 226, 1724–1742, 2013.

Brown, R. D. and Mote, P. W.: The response of Northern Hemisphere snow cover to a changing climate, Journal of Climate, 22, 2124–2145, 2009.

cemcer.it: www.cemcer.it, last access: 26/07/2020.

Centro Funzionale Mutlirischi Regione Campania, A. I.: Annali Idrologici, Centro Funzionale Mutlirischi per la Meteorologia, l'Idrologia e la Sismologia Regione Capania.

Centro Funzionale Mutlirischi Regione Marche, A. I.: Annali Idrologici, Centro Funzionale Mutlirischi per la Meteorologia, l'Idrologia e la Sismologia Regione Marche.

Centro Meteorologico Lombardo, A. I.: Annali Idrologici, Centro Meteorologico Lombardo.

Cohen, J., Screen, J. A., Furtado, J. C., Barlow, M., Whittleston, D., Coumou, D., Francis, J., Dethloff, K., Entekhabi, D., Overland, J., et al.: Recent Arctic amplification and extreme mid-latitude weather, Nature geoscience, 7, 627–637, 2014.

Cohen, J., Zhang, X., Francis, J., Jung, T., Kwok, R., Overland, J., Ballinger, T., Bhatt, U., Chen, H., Coumou, D., et al.: Divergent consensuses on Arctic amplification influence on midlatitude severe winter weather, Nature Climate Change, 10, 20–29, 2020.

Collegio Alberoni Piacenza, O. M.: Osservatorio Meteorologico del Collegio Alberoni of Piacenza.

Corriere, d. M.: Febbraio 1956: sul Lungomare si poteva addirittura sciare., Corriere del mezzogiorno of 07/02/2011.

Corriere, d. S.: Neve e vento, l'Italia gela., Corriere della Sera of 03/01/1993.

Corriere, d. S.: Scosse, neve, dispersi., Corriere della Sera of 19/01/2017.

Corriere, d. S.: Neve nel Centro-sud: traffico in tilt., Corriere della Sera of 25/01/2005.

Coumou, D. and Rahmstorf, S.: A decade of weather extremes, Nature climate change, 2, 491–496, 2012.

de Vries, H., Woollings, T., Anstey, J., Haarsma, R. J., and Hazeleger, W.: Atmospheric blocking and its relation to jet changes in a future climate, Climate dynamics, 41, 2643–2654, 2013.

Defrance, D., R. G. C. S. V. M. A. M. S. B. S. D. D. C. G. F. A.-S. J. and Vanderlinden, J.-P.: Consequences of rapid ice-sheet melting on the Sahelian population vulnerability, Proceedings of the National Academy of Sciences of the United States of America (PNAS), 114, 6533 – 6538, https://doi.org/10.1073/pnas.1619358114, 2017.

Delle Acque, O. M.: Osservatorio delle Acque.

Déqué, M.: Frequency of precipitation and temperature extremes over France in an anthropogenic scenario: Model results and statistical correction according to observed values, Global Planet. Change, 57, 16 – 26, 2007.

Deser, C., Hurrell, J. W., and Phillips, A. S.: The role of the North Atlantic Oscillation in European climate projections, Climate dynamics, 49, 3141–3157, 2017.

Di Palermo, O. A.: Osservatorio Astronomico di Palermo.

Diodato, N.: Montevergine: unica vedetta storica dell'Appennino fondata per mezzo di padre Francesco Denza, Boll Geof, 3, 47–51, 1995.

Diodato, N., Büntgen, U., and Bellocchi, G.: Mediterranean winter snowfall variability over the past millennium, International Journal of Climatology, 39, 384–394, 2019.

Easterling, D. R., Meehl, G. A., Parmesan, C., Changnon, S. A., Karl, T. R., and Mearns, L. O.: Climate extremes: observations, modeling, and impacts, science, 289, 2068–2074, 2000.

Eichler, W.: Strenge Winter 1962/1963 und seine vielschichtigen biologischen Auswirkungen in Mitteleuropa., Vienna Zool bot Ges Verh, 1971.

evalmet.it: www.evalmet.it, last access: 26/07/2020.

Fabiano, F., Meccia, V. L., Davini, P., Ghinassi, P., and Corti, S.: A regime view of future atmospheric circulation changes in northern mid-latitudes, Weather and Climate Dynamics, 2, 163–180, 2021.

Falkena, S. K., de Wiljes, J., Weisheimer, A., and Shepherd, T. G.: Revisiting the identification of wintertime atmospheric circulation regimes in the Euro-Atlantic sector, Quarterly Journal of the Royal Meteorological Society, 146, 2801–2814, 2020.

Faranda, D.: An attempt to explain recent trends in European snowfall extremes, Weather and Climate Dynamics, 2, 1–14, https://doi.org/doi.org/10.5194/wcd-2-1-2020, 2020.

Faranda, D., Messori, G., and Yiou, P.: Dynamical proxies of North Atlantic predictability and extremes, Scientific reports, 7, 41 278, 2017.

Faranda, D., Vrac, M., Yiou, P., Jézéquel, A., and Thao, S.: Changes in future synoptic circulation patterns: consequences for extreme event attribution, Geophysical Research Letters, 47, e2020GL088 002, 2020.

firenzemeteo.net: www.firenzemeteo.net, last access: 26/07/2020.

Fraedrich, K. and Lunkeit, F.: Diagnosing the entropy budget of a climate model, Tellus A: Dynamic Meteorology and Oceanography, 60, 921–931, 2008.

Fraedrich, K., Jansen, H., Kirk, E., Luksch, U., and Lunkeit, F.: The Planet Simulator: Towards a user friendly model, Meteorologische Zeitschrift, 14, 299–304, 2005a.

Fraedrich, K., Kirk, E., Luksch, U., and Lunkeit, F.: The portable university model of the atmosphere (PUMA): Storm track dynamics and low-frequency variability, Meteorologische Zeitschrift, 14, 735–745, 2005b.

Francis, J. A. and Vavrus, S. J.: Evidence linking Arctic amplification to extreme weather in mid-latitudes, Geophysical research letters, 39, 2012.

Genio Civile Bari, A. I.: Annali Idrologici Genio Civile Bari.

Genio Civile Catanzaro, A. I.: Annali Idrologici Genio Civile Catanzaro.

Genio Civile Napoli, A. I.: Annali Idrologici Genio Civile Napoli.

Genio Civile Palermo, A. I.: Annali Idrologici Genio Civile Palermo.

Genio Civile Pescara, A. I.: Annali idrologici Sezione Autonoma del Genio Civile Pescara.

Genio Civile Pisa, A. I.: Annali Idrologici Genio Civile Pisa.

Giornale di, S.: Neve a Messina., Giornale di Sicilia 7/01/1981.

Grazzini, F.: Cold spell prediction beyond a week: extreme snowfall events in February 2012 in Italy, ECMWF Newsl, 136, 31–35, 2013.

Gudmundsson, L., Bremnes, J. B., Haugen, J. E., and Engen-Skaugen, T.: Downscaling RCM precipitation to the station scale using statistical transformations–a comparison of methods, Hydrology and Earth System Sciences, 16, 3383–3390, 2012.

Haddad, Z. and Rosenfeld, D.: Optimality of empirical z-r relations, Q. J. R. Meteorol. Soc., 123, 1283–1293, 1997.

Hamouda, M. E., Pasquero, C., and Tziperman, E.: Decoupling of the Arctic Oscillation and North Atlantic Oscillation in a warmer climate, Nature Climate Change, 11, 137–142, 2021.

Il.Foglio: Neve a Roma., Il Foglio 26/02/2017.

Il.Mattino: Il meteorologo: A Napoli neve così solo nel '56., Il Mattino of 27/02/2018.

Il.Messaggero: Temperature polari in Ciociaria., Il Messaggero 17/12/2010.

Il.Quotidiano: Nevicate, ghiaccio e gelo Treni e aerei nel caos Milano quasi paralizzata. La Russa manda l'esercito., Il Quotidiano 19/12/2009.

James, F.: The Weather and circulation of January 1963, Monthly Weather Review, 1963.

Jézéquel, A., Yiou, P., and Radanovics, S.: Role of circulation in {European} heatwaves using flow analogues, Climate Dynamics, https://doi.org/10.1007/s00382-017-3667-0, 2018.

Jordan-Bychkov, Terry G., B. B. J. and Murphy, A. B.: The European culture area: A systematic geography., Rowman & Littlefield Publishers, 2008.

Kawase, H., Murata, A., Mizuta, R., Sasaki, H., Nosaka, M., Ishii, M., and Takayabu, I.: Enhancement of heavy daily snowfall in central Japan due to global warming as projected by large ensemble of regional climate simulations, Climatic Change, 139, 265–278, 2016.

La.Gazzetta, d. P.: Freddo e neve anche a quote basse: Big snow., La Gazzetta di Parma 14/02/2018.

La.Gazzetta, d. S.: La prima neve all'Abetone., La Gazzetta del Serchio 22/02/2018.

La.Nazione: Aria gelida dal Nord Europa., La Nazione of 11/11/1968.

La.Repubblica: Arrivano i giorni del gelo neve a bassa quota così i piani d'emergenza., La Repubblica 05/01/2017.

La.Repubblica: Nevicata a Roma, Castelli imbiancati, Freddo e maltempo in tutta Italia., La Repubblica 12/02/2010.

La.Repubblica: Il gelo arriva in Sicilia: neve a Palermo., La Repubblica 12/02/2012.

La.Repubblica: La neve congela il Nord Genova, la città si blocca., La Repubblica 17/01/2001.

La.Repubblica: Neve e gelo in Campania giù le temperature in città., La Repubblica 17/01/2016.

La.Repubblica: Neve e gelo artico da Nord a Sud sarà il weekend più freddo dell' anno., La Repubblica 19/12/2009.

La.Repubblica: Neve e gelo, il grande freddo di Natale; Roma sotto zero, neve in tutt'Italia., La Repubblica 27/12/1996 and 28/12/1996.

La.Repubblica: Da oggi gelo e neve sull'Italia allerta-meteo in sei Regioni., La Repubblica 27/12/2014.

La.Repubblica: Neve, disagi e impreparazione., La Repubblica Bologna 10/02/2015.

La.Repubblica: L'Europa sottozero., La Repubblica of 02/02/1991.

La.Repubblica: Corsa contro l'inverno., La Repubblica of 12/03/1987.

La.Repubblica: Il gelo assedia il Centro-Sud., La Repubblica of 13/12/2007.

La.Repubblica: In trappola senza cibo né gasolio., La Repubblica of 24/02/1999.

La.Stampa: Neve a Roma, non accadeva dal 2005., La Stampa of 12/02/2010.

La.Stampa: Roma traffico paralizzato anche i telefoni interrotti., La Stampa of 6-7/03/1971.

Lazio, Protezione Civile, A. I.: Agenzia Regionale Protezione Civile Lazio Annali Idrologici.

Lazio, A. R.: www.dati.lazio.it, ARSIAL: Agenzia Regionale per lo Sviluppo e l'Innovazione dell'Agricoltura del Lazio, last access: 26/07/2020.

Lehmann, J. and Coumou, D.: The influence of mid-latitude storm tracks on hot, cold, dry and wet extremes, Scientific reports, 5, 17 491, 2015.

Le.Parisien: C'est la Sibérie!, Le Parisien 03/01/1997.

Liu, J., Curry, J. A., Wang, H., Song, M., and Horton, R. M.: Impact of declining Arctic sea ice on winter snowfall, Proceedings of the National Academy of Sciences, 109, 4074–4079, 2012.

livesicilia.it: www.livesicilia.it, last access: 26/07/2020.

Lucarini, V., Fraedrich, K., and Lunkeit, F.: Thermodynamic analysis of snowball earth hysteresis experiment: efficiency, entropy production and irreversibility, Quarterly Journal of the Royal Meteorological Society: A journal of the atmospheric sciences, applied meteorology and physical oceanography, 136, 2–11, 2010a.

Lucarini, V., Fraedrich, K., and Lunkeit, F.: Thermodynamics of climate change: Generalized sensitivities, Atmos. Chem. Phys, 10, 9729–9737, 2010b.

Lucarini, V., Faranda, D., and Wouters, J.: Universal behaviour of extreme value statistics for selected observables of dynamical systems, Journal of statistical physics, 147, 63–73, 2012.

Lucarini, V., Blender, R., Herbert, C., Ragone, F., Pascale, S., and Wouters, J.: Mathematical and physical ideas for climate science, Reviews of Geophysics, 52, 809–859, 2014.

Mangianti, F. and Beltrano, M.: La neve a Roma dal 1741 al 1990, vol. pp 55, UCEA, 1991.

Maraun, D.: Bias correcting climate change simulations-a critical review, Current Climate Change Reports, 2, 211–220, 2016.

Marty, C. and Blanchet, J.: Long-term changes in annual maximum snow depth and snowfall in Switzerland based on extreme value statistics, Climatic Change, 111, 705–721, 2012.

Mercalli, L. and Berro, D. C.: Atlante climatico della Valle d'Aosta, vol. 2, SMS, 2003.

meteo net: www.meteo-net.it, last access: 26/07/2020.

meteo.ansa.it: www.meteo.ansa.it, last access: 26/07/2020.

meteociel.fr: www.meteociel.fr, last access: 26/07/2020.

meteogiornale.it: www.meteogiornale.it, last access: 26/07/2020.

meteolanguedoc.com: www.meteolanguedoc.com, last access: 26/07/2020.

meteolive.it: www.meteolive.it, last access: 26/07/2020.

meteopalermo.it: www.meteopalermo.it, last access: 26/07/2020.

meteoservice.net: www.meteoservice.net, last access: 26/07/2020.

meteosicilia.it: www.meteosicilia.it, last access: 26/07/2020.

meteoweb.eu: www.meteoweb.eu, last access: 26/07/2020.

Michelangeli, P., Vrac, M., and Loukos, H.: Probabilistic downscaling approaches: application to wind cumulative distribution functions, Geophys. Res. Lett., 36, L11 708, https://doi.org/10.1029/2009GL038401, https://agupubs.onlinelibrary.wiley.com/doi/full/10.1029/2009GL038401, 2009.

Michelangeli, P.-A., Vautard, R., and Legras, B.: Weather regimes: Recurrence and quasi stationarity, Journal of the atmospheric sciences, 52, 1237–1256, 1995.

Milano.Repubblica: Il giorno del grande freddo., Milano Repubblica 11/02/2013.

milanotoday.it: www.milanotoday.it, last access: 26/07/2020.

Murakami, M., Clark, T. L., and Hall, W. D.: Numerical simulations of convective snow clouds over the sea of Japan, Journal of the Meteorological Society of Japan. Ser. II, 72, 43–62, 1994.

Nguyen, H., Mehrotra, R., and Sharma, A.: Correcting for systematic biases in GCM simulations in the frequency domain, Journal of Hydrology, 538, 117–126, 2016.

Nicolet, G., Eckert, N., Morin, S., and Blanchet, J.: Decreasing spatial dependence in extreme snowfall in the French Alps since 1958 under climate change, Journal of Geophysical Research: Atmospheres, 121, 8297–8310, 2016.

Nicolet, G., Eckert, N., Morin, S., and Blanchet, J.: Assessing climate change impact on the spatial dependence of extreme snow depth maxima in the French Alps, Water Resources Research, 54, 7820–7840, 2018.

nimbus.it: www.nimbus.it, last access: 26/07/2020.

Oettli, P., Sultan, B., Baron, C., and Vrac, M.: Are regional climate models relevant for crop yield prediction in West Africa ?, Environ. Res. Lett., 6, https://doi.org/10.1088/1748-9326/6/1/014008, 2011.

Overland, J. E. and Wang, M.: Large-scale atmospheric circulation changes are associated with the recent loss of Arctic sea ice, Tellus A: Dynamic Meteorology and Oceanography, 62, 1–9, 2010.

O'Gorman, P. A.: Contrasting responses of mean and extreme snowfall to climate change, Nature, 512, 416–418, 2014.

Pachauri, R. K., Allen, M. R., Barros, V. R., Broome, J., Cramer, W., Christ, R., Church, J. A., Clarke, L., Dahe, Q., Dasgupta, P., et al.: Climate change 2014: synthesis report. Contribution of Working Groups I, II and III to the fifth assessment report of the Intergovernmental Panel on Climate Change, Ipcc, 2014.

palermotoday.it: https://www.palermotoday.it/cronaca/neve-palermo-14-febbraio-2012.html, last access: 26/07/2020.

Panofsky, H. and Brier, G.: Some Applications of Statistics to Meteorology, Tech. rep., University Park, Penn. State Univ., 1958.

Payne, G. and Payne, J.: Key concepts in social research, Sage, 2004.

Peings, Y., Cattiaux, J., and Douville, H.: Evaluation and response of winter cold spells over Western Europe in CMIP5 models, Climate dynamics, 41, 3025–3037, 2013.

Pons, F. M. E., Messori, G., Alvarez-Castro, M. C., and Faranda, D.: Sampling hyperspheres via extreme value theory: implications for measuring attractor dimensions, Journal of statistical physics, 179, 1698–1717, 2020.

protezionecivile.puglia.it: www.protezionecivile.puglia.it, last access: 26/07/2020.

Puglia, P. C.: Protezione Civile Puglia.

Ragone, F., Wouters, J., and Bouchet, F.: Computation of extreme heat waves in climate models using a large deviation algorithm, Proceedings of the National Academy of Sciences, 115, 24–29, 2018.

Randi, P. and Ghiselli, R.: I Grandi Inverni dal 1880 in Romagna e Province di Bologna e Ferrara, An. Walberti, 2013.

recordmeteo.altervista.org: www.recordmeteo.altervista.org, last access: 26/07/2020.

Regione Abruzzo, D. P. d. S. R. e. d.: Regione Abruzzo Dipartimeto Politiche dello Sviluppo Rurale e dell'Ambiente.

Regione Abruzzo, S. P. T. d. S. a. S. A.: Regione Abruzzo, Servizio Presidi Tecnici di Supporto al Settore Agricolo.

Regione Toscana, S. I. R.: www.sir.toscana.it, Servizio Idrologico Regionale Regione Toscana, last access: 26/07/2020.

regione.abruzzo.it: www.regione.abruzzo.it, last access: 26/07/2020.

Resto, d. C.: Crolli a Modena, Parma e Genova causati dall'eccezionale nevicata, Resto del Carlino 05/01/1954.

Resto, d. C.: Nevicate nel novembre 1979., Resto del Carlino 13/11/1979.

Riahi, K., Rao, S., Krey, V., Cho, C., Chirkov, V., Fischer, G., Kindermann, G., Nakicenovic, N., and Rafaj, P.: RCP 8.5—A scenario of comparatively high greenhouse gas emissions, Climatic Change, 109, 33, 2011.

roma artigiana.it: www.roma-artigiana.it, last access: 26/07/2020.

Roscher, M., Stordal, F., and Svensen, H.: The effect of global warming and global cooling on the distribution of the latest Permian climate zones, Palaeogeography, Palaeoclimatology, Palaeoecology, 309, 186–200, 2011.

Sardegna, A. I.: Annali Idrologici della Sardegna.

Screen, J. A.: The missing Northern European winter cooling response to Arctic sea ice loss, Nature communications, 8, 1–9, 2017.

Serquet, G., Marty, C., Dulex, J.-P., and Rebetez, M.: Seasonal trends and temperature dependence of the snowfall/precipitation-day ratio in Switzerland, Geophysical research letters, 38, 2011.

severe weather.eu: www.severe-weather.eu, last access: 26/07/2020.

Shrestha, M., Acharya, S. C., and Shrestha, P. K.: Bias correction of climate models for hydrological modelling–are simple methods still useful?, Meteorological Applications, 24, 531–539, 2017.

sienanews.it: www.sienanews.it, last access: 26/07/2020.

Steiger, S. M., Hamilton, R., Keeler, J., and Orville, R. E.: Lake-effect thunderstorms in the lower Great Lakes, Journal of Applied Meteorology and Climatology, 48, 889–902, 2009.

Stocchi, P. and Davolio, S.: Intense air-sea exchanges and heavy orographic precipitation over Italy: The role of Adriatic sea surface temperature uncertainty, Atmospheric Research, 196, 62–82, 2017.

Strong, C., Magnusdottir, G., and Stern, H.: Observed feedback between winter sea ice and the North Atlantic Oscillation, Journal of Climate, 22, 6021–6032, 2009.

Taylor, K. E., Stouffer, R. J., and Meehl, G. A.: An overview of CMIP5 and the experiment design, Bulletin of the American Meteorological Society, 93, 485–498, 2012.

Teutschbein, C. and Seibert, J.: Bias correction of regional climate model simulations for hydrological climate-change impact studies: Review and evaluation of different methods, Journal of hydrology, 456, 12–29, 2012.

Teutschbein, C. and Seibert, J.: Is bias correction of regional climate model (RCM) simulations possible for non-stationary conditions?, Hydrology and Earth System Sciences, 17, 5061–5077, 2013.

thamesweb.co.uk: www.thamesweb.co.uk, last access: 26/07/2020.

Tibaldi, S. and Buzzi, A.: Effects of orography on Mediterranean lee cyclogenesis and its relationship to European blocking, Tellus A: Dynamic Meteorology and Oceanography, 35, 269–286, 1983.

today.it: www.today.it, last access: 26/07/2020.

Troin, M., Vrac, M., Khodri, M., Caya, S., Vallet-Coulomb, C., Piovano, E., and Sylvestre, F.: A complete hydro-climate model chain to investigate the influence of sea surface temperature on recent hydroclimatic variability in subtropical South America (Laguna Mar Chiquita, Argentina), Climate Dynamics, 46, 2015.

Ufficio Idrografico del Po, A. I.: Annali Idrologici Ufficio Idrografico del Po.

Ufficio Idrografico di Roma, A. I.: Ufficio Idrografico di Roma.

Ufficio Idrografico di Venezia, A. I.: Annali Idrologici Ufficio Idrografico Magistrato delle Acque di Venezia.

Ufficio Idrografico e Mareografico di Bari, A. I.: Annali Ufficio Idrografico e Mareografico di Bari.

Ufficio Idrografico e Mareografico di Parma, A. I.: Annali Idrologici Ufficio Idrografico e Mareografico di Parma.

Ufficio Idrografico e Mareografico di Pesacra, A. I.: Annali Idrologici Servizio Idrografico e Mareografico di Pescara.

Ufficio Idrografico e Mareografico di Pisa, A. I.: Annali Ufficio Idrografico e Mareografico di Pisa.

Ufficio Idrografico e Mareografico di Roma, A. I.: Annali Ufficio Idrografico e Mareografico di Roma.

Ufficio Idrografico e Mareografico di Venezia, A. I.: Annali Idrologici Ufficio Idrografico e Mareografico di Venezia.

valdarnopost.it: www.valdarnopost.it, last access: 26/07/2020.

Van Vuuren, D. P., Edmonds, J., Kainuma, M., Riahi, K., Thomson, A., Hibbard, K., Hurtt, G. C., Kram, T., Krey, V., Lamarque, J.-F., et al.: The representative concentration pathways: an overview, Climatic change, 109, 5, 2011a.

Van Vuuren, D. P., Edmonds, J., Kainuma, M., Riahi, K., Thomson, A., Hibbard, K., Hurtt, G. C., Kram, T., Krey, V., Lamarque, J.-F., et al.: The representative concentration pathways: an overview, Climatic change, 109, 5–31, 2011b.

Van Vuuren, D. P., Kriegler, E., O'Neill, B. C., Ebi, K. L., Riahi, K., Carter, T. R., Edmonds, J., Hallegatte, S., Kram, T., Mathur, R., et al.: A new scenario framework for climate change research: scenario matrix architecture, Climatic Change, 122, 373–386, 2014.

Vavrus, S., Walsh, J., Chapman, W., and Portis, D.: The behavior of extreme cold air outbreaks under greenhouse warming, International Journal of Climatology: A Journal of the Royal Meteorological Society, 26, 1133–1147, 2006.

Vigaud, N., Vrac, M., and Caballero, Y.: Probabilistic downscaling of GCM scenarios over southern India, International journal of climatology, 33, 1248–1263, 2013.

Volosciuk, C. D., Maraun, D., Vrac, M., and Widmann, M.: A combined statistical bias correction and stochastic downscaling method for precipitation, Hydrology and Earth System Sciences, 21, 1693–1719, 2017.

Vrac, M., Drobinski, P., Merlo, A., Herrmann, M., Lavaysse, C., Li, L., and Somot, S.: Dynamical and statistical downscaling of the French Mediterranean climate: uncertainty assessment, Natural Hazards and Earth System Sciences, 12, 2769–2784, https://doi.org/10.5194/nhess-12-2769-2012, https://www.nat-hazards-earth-syst-sci.net/12/2769/2012/, 2012.

Vrac, M., Noël, T., and Vautard, R.: Bias correction of precipitation through Singularity Stochastic Removal: Because occurrences matter, Journal of Geophysical Research: Atmospheres, 121, 5237–5258, 2016.

Wetterzentrale.de: www.Wetterzentrale.de, last access: 26/07/2020.

WMO: International Meteorological Vocabulary: Vocabulaire Météorologique International. Vocabulario Meteorológico Internacional, Secretariat of the World Meteorological Organization, 1966.

Wu, Q. and Zhang, X.: Observed forcing-feedback processes between Northern Hemisphere atmospheric circulation and Arctic sea ice coverage, Journal of Geophysical Research: Atmospheres, 115, 2010.

Yiou, P., Salameh, T., Drobinski, P., Menut, L., Vautard, R., and Vrac, M.: Ensemble reconstruction of the atmospheric column from surface pressure using analogues, Climate dynamics, 41, 1333–1344, 2013.

Zscheischler, J., Martius, O., Westra, S., Bevacqua, E., Raymond, C., Horton, R. M., van den Hurk, B., AghaKouchak, A., Jézéquel, A., Mahecha, M. D., et al.: A typology of compound weather and climate events, Nature reviews earth & environment, pp. 1–15, 2020.

Appendix A: Description of detected Events

In this section, we describe each extreme cold event selected as a cold spell in this study. The mains characteristics of the events are the occurrence of snowfalls in regions where snow cover has usually been rare or absent since a long time (e.g. lowlands and coasts), large socioeconomic impacts (e.g. in 2017), extreme minimum temperatures, and extreme amount of snowfalls. The date reported at the beginning of each event is the one selected as the most representative day of each ~~cold spell~~ cold spell event and it is the one used for the analogues search. The information about the duration of the events are reported in the text for each description.

1) 4th January 1954. A cold spell rapidly built in the Mediterranean in January 1954 (an exceptional month in Spain). Heavy snowfalls affected all of northern Italy, including lowland areas in the Po Valley. In 24 hours, 60 cm of snow fell over Turin, Brescia, Milano, Piacenza, Cremona, Reggio Emilia, Bologna and Vicenza (-5°C at 1400 m Osservatorio Meteorologico del Collegio Alberoni of Piacenza) according to information found in the press (Resto del Carlino 05/01/1954). Traffic disruption occurred mainly in Piacenza and Cremona (daily local journal of Cremona 06/01/1954).

2) 4th February 1956. One of the coldest and snowiest events of the 20th century in Europe. The -15°C isotherm at 850 hPa was located above the Po Valley (1-2/02/1956 Wetterzentrale.de (last access: 26/07/2020)); snow storms affected the entire country, with a historical snowfall in Rome. A powerful extratropical cyclone embedded in very cold mid-tropospheric air core struck the Southern regions causing heavy snowfalls in Rome and throughout central and Southern Italy, with blizzards and heavy frost. Significant snowfall was reported even on the Sicilian coast: in Palermo, the minimum temperature dropped to 0° C (daily data of Palermo and Sicily on 1956, ANNALI/A1956) and the city was blanketed by several centimeters of snow, which also fell on the southern coasts of Sicily and the island of Lampedusa (Corriere del mezzogiorno of 07/02/2011).

3) 17th December 1961. December was a very cold month for most of Italy with a historical snowfall in southern Italy coastal areas as in Bari (30 cm, Protezione Civile Puglia of 17/12/1961). After 3 days of heavy snowfall, a record snow height of 370 cm was reported in Roccacaramanico (1050 m above sea level on the East side of the Central Appennini) on December 20 (Annali idrologici Sezione Autonoma del Genio Civile Pescara 12/1961), and all the Adriatic regions were affected by heavy snowfalls (meteogiornale.it (last access: 26/07/2020) of 18-12-2014).

4) 31st January 1962. Sicily reported several historical records of daily low temperature as in Lentini città (-2.5°C), Caltanissetta (-4.5°C), Caltagirone (-3.2°C), Castronovo di Sicilia/Piano del Leone (-8.5°C)(Osservatorio delle Acque 01-02/1962). Heavy snowfall occurred on the North coast, in Palermo and Capo d'Orlando (meteolive.it (last access: 26/07/2020) of 28/02/2002, meteosicilia.it (last access: 26/07/2020) of 07/12/2007).

5) 22nd January 1963. Winter 1963 was one of the coldest in Western European records. Sea frost trapped Norway's islanders, while a record low temperature of -41.2°C was recorded in Northern Sweden village of Karesuando. Average temperatures for the month were in excess of -5°C below normal from southern England across Europe to the Urals. Warsaw reported an average temperature of -12.4°C for January, while Paris averaged -5.5°C below normal. Mediterranean regions averaged about -3°C below normal (James, 1963). The upper reaches of the Thames river froze thamesweb.co.uk (last access: 26/07/2020) and the lowest temperature in Germany was measured on January 2 at Quedlinburg at -30.2°C (Eichler, 1971). In Italy the temperature drop was brought by strong bora winds (110 km/h, Annali Idrologici Ufficio Idrografico del Po 01/1963) and snow accumulation over Friuli-Venezia Giulia (5 cm to 10 cm) reaching Venezia, where the Lagoon also froze. Very low temperatures (Trieste: -9°C, Udine: -10°C, Pordenone -15°C, Milano: -8°C, Bologna -7°C, Annali Idrologici Ufficio Idrografico del Po, Arpae.it (last access: 26/07/2020) 01/1963) affected all other regions of Italy, with snowstorms over Toscana, Marche, Abruzzo, Molise, Apulia, and several cities were completely isolated (meteogiornale.it (last access: 26/07/2020) of 21/01/2011, Randi and Ghiselli (2013), regione.abruzzo.it (last access: 26/07/2020); protezionecivile.puglia.it (last access: 26/07/2020) 01/1963).

6) 12th January 1968. Between the 9th and the 15th January 1968, Tuscany and nearby areas were affected by one of the strongest cold spells on record for the region. Extreme daily low temperatures were recorded: Città di Castello (Umbria, 295 m, Ufficio Idrografico di Roma) -23°C, Arezzo (S. Fabiano) (277 m) -14.2°C, Verghereto (812 m) -15.2°C, Cortona (393 m) -8.7°c (Annali Idrologici Genio Civile Pisa 01/1968). Heavy snowfall affected the area, with snow depth measuring: 65 cm in Eremo di Camaldoli (1111 m above sea level), 60 cm in Verghereto (812 m a.s.l.) , 15 cm in Arezzo (S. Fabiano) (277 m a.s.l.), and 19 cm in Florence (Ximenian Observatory, 51 m a.s.l.) (Annali Idrologici Genio Civile Pisa 01/1968); (La Nazione of 11/11/1968).

7) 28th February 1971. On February 24, the presence of an omega blocking with an anticyclone meridionally elevated towards the British isles and a trough with a pressure minimum over Central Mediterranean, triggered a flow of Arctic air towards the Mediterranean. After affecting Northern Europe, the cold spell reached Italy, causing a severe temperature drop between February 28 and March 1. On the morning of March 1st, almost all of Italy recorded minimum temperatures below zero even in lowland and coastal areas: -5°C in Florence and Pisa (Annali Idrologici Genio Civile Pisa), -4°C in Rome (Ardea, Ufficio Idrografico di Roma 02/1971), -1°C in Naples (Annali Idrologici Genio Civile Napoli 02/1971) with a snowfall that also reached the coastal areas of the city (La Stampa of 6-7/03/1971).

8) 1st December 1973. At the beginning of December, a cold air mass associated to a low pressure area reached Italy from Scandinavia, with the -15°C isotherm located over the Alps. Cold conditions persisted for long time, yelding to low minimum temperatures during the first two weeks of December, reaching -7°C in Novara, Treviso and Arezzo, -6°C in Udine and Potenza, -5°C in Foggia, -2°C in Trieste, and -19°C on Monte Cimone (2173 m a.s.l.), where North-Easterly wind at 133km/h was also recorded. Due to these conditions, highways remained closed in Tuscany for half a day, disrupting im-

portant road networks. Snow fell in Florence, (17 cm), and Valle del Serchio received 30 cm of snow, after around 40 years during which snow was almost absent. Snow accumulations ($\approx$15 cm) was also recorded in Perugia, Gubbio, Assisi, Spoleto, Sangemini (sienanews.it (last access: 26/07/2020) 13/12/2016, Annali Idrologici Ufficio Idrografico Magistrato delle Acque di Venezia.; Annali Idrologici Genio Civile Pisa; Annali Idrologici Genio Civile Catanzaro; Annali Idrologici Genio Civile Bari; Annali Idrologici Ufficio Idrografico del Po, Arpae.it (last access: 26/07/2020), 12/1973, Aeronautica.Militare (last access: 26/07/2020)).

9) 15th January 1979. A large pool of Arctic air stretching up to the North African coasts brought a cold spell that affected most of Europe, causing several fatalities. The cold air caused wind storms in the Thyrrenian Sea, followed by a severe temperature drop. Snowfall occurred in Tuscany (Annali Idrologici Genio Civile Pisa 01/1979), Sardinia and most of Central and Southern Italy, with snowstorms in the Marche, Abruzzo, Molise (regione.abruzzo.it (last access: 26/07/2020)) and Basilicata (evalmet.it (last access: 26/07/2020)) regions. The most abundant snowfalls were observed on January 19 with the advection of more temperate and humid air from the South-West. Traffic problems due to frost on the roads and to iced pipes were reported (Resto del Carlino 13/11/1979).

10) 8th January 1981. An very cold air mass penetrated deeply in the Central Mediterranean Sea, accompanied by an intense storm over the South of Italy. On January 8, Western-Central Sicily was disrupted by unprecedented amounts of snow for the area, with 30 cm of snowfall even on the coasts. Extremely unusual snowfall was observed even on Pantelleria, a small island located South of Sicily, with only 5 m elevation above sea level. Some cities in the provinces of Palermo, Trapani, Messina and Enna, remained isolated for days. Temperature reached a historical minimum of -0.5°C in Palermo, where continuous snow precipitations for more than 24 hours are an exceptional event (Giornale di Sicilia 7/01/1981, meteolive.it (last access: 26/07/2020) of 28/02/2002, Annali Idrologici Genio Civile Palermo 01/1981).

11) 7th January 1985. From 1st to 17th January 1985, Italy and most of Western Europe were affected by a disruptive and persistent cold spell. A cyclogenesis over Central Italy, between Tuscany and Lazio, triggered strong Bora winds and historical snowfalls that affected Florence with 40 cm of accumulation (up to 80 cm in Val di Cecina) and Rome with 30 cm. The pressure minimum moved towards the South-East between the 6th and 9th January, and the snow reached also Campania and the rest of the South with accumulations up to 25 cm on the hilly zones of Naples, as it had not happened since 1956 (Annali Idrologici Genio Civile Napoli 07/1985). Between January 1 and 11th temperature records were broken in the minimum values in Florence (Peretola, -23.2°C) and Piacenza (S. Damiano, -22.2°C). The Northern regions were particularly affected a few days later, between January 14 and 17: temperatures around -20°C were registered in the Po Valley, and exceptional snowfalls disrupted traffic and industrial activities in the cities of the North, including Milan, with historical accumulations. (Aeronautica.Militare (last access: 26/07/2020); valdarnopost.it (last access: 26/07/2020) of 14.01.2015, Il Mattino of 27/02/2018, firenzemeteo.net (last access: 26/07/2020) of 19/01/2017).

12) 24th December 1986. Christmas day 1986 was characterized by strong winds and 850 hPa isotherms of -10°C that covered most of Italian Peninsula (meteociel.fr (last access: 26/07/2020) 25/12/1986). In Pescara, on the evening of December 26, the temperature reached -9°C and about 15 cm of snow fell. Snowfall affected the entire Adriatic side of the country (5 cm in Perugia, more than 30 cm in Molise). In Ancona (Falconara) wind gusts exceeded 95 km/h with a minimum temperature of

-6°C (Aeronautica.Militare, last access: 26/07/2020). The snow then reached Sardinia and even Apulia, where the temperature in Bari dropped to -1°C (Annali Idrologici Genio Civile Bari 12/1986). A record low temperature for December was measured in Pantelleria, with 2.6°C on December 25 (Annali Idrologici Genio Civile Palermo 12/1986, meteolive.it (last access: 26/07/2020) of 31/01/2008, meteogiornale.it (last access: 26/07/2020) of 31/12/2014).

13) 03rd March 1987. Cold air and stormy weather reached the extreme South-East of Italy, with a peak on 8th March 1987 when the -12°C 850 hPa isotherm covered the whole of Apulia (Annali Idrologici Genio Civile Bari 03/1987). Snow fell on the Southern cities of Naples, Crotone and even in Palermo. Impressive snow accumulations were recorded on those days: in Gioia del Colle snowfall reached 72 cm, for a total of 9 days of permanence of snow on the ground, exceptional for the area (Annali Idrologici Genio Civile Bari 03/1987, 3bmeteo.com (last access: 26/07/2020) of 08/03/2019; La Repubblica of 12/03/1987, meteogiornale.it (last access: 26/07/2020) of 13-03-2005).

14) 31st January 1991. Cold air entered the Mediterranean as strong Bora winds, causing temperature to drop to -4.2°C in Trieste (Annali Idrologici Ufficio Idrografico e Mareografico di Venezia 01-02/1991). Snow fell on Bologna, Rimini, Forlì, and eventually on the Marche coastal area, with 5 cm of accumulation in the harbour city of Ancona. The cold air mass also spreaded West over the Po Valley, from Veneto to Piemonte, with widespread snowfalls. Minimum temperatures of -21.2°C were recorded at Passo Rolle, -12°C in Novara, -11.6°C in Bologna (Aeronautica.Militare, last access: 26/07/2020). February 7 is one of the coldest (Annali Idrologici Ufficio Idrografico e Mareografico di Venezia; Annali Idrologici Ufficio Idrografico e Mareografico di Parma 01-02/1991) days in the history of Northern and Central Italian climatology (Randi and Ghiselli (2013), meteoservice.net (last access: 26/07/2020) of 05/02/2016, recordmeteo.altervista.org (last access: 26/07/2020) of 01/03/2012, La Repubblica of 02/02/1991).

15) 1st January 1993. A zonally tilted anticyclone with pressure maxima between the UK and Scandinavia draw a large Arctic air patch, from Russia towards Italy. Due to the peculiar configuration, cold air flowed from Russia through Ukraine, Romania and the Balkans, then mostly affecting Southern and Central Italian regions, especially the Adriatic side, where the snow fell also in coastal areas. The absolute minimum temperature record was broken in Bari (-5.9°C) (Aeronautica.Militare, last access: 26/07/2020). Snow fell in the southern part of the Italian peninsula and Sicily (Reggio Calabria and Messina), but also on the Po Valley (Parma, Modena, Reggio Emilia), on the Adriatic coast, from Rimini to Cattolica, and in Tuscany. Snowfall was also observed in the Northern part of the Rome metropolitan area. Snowfall affected the Thyrrenian and Adriatic sides of Italy simultaneously, which is rare. The cold air moving westward then caused additional extensive snowfalls in the North and Central Italy. Intense cold conditions persisted for a long time in the Po Valley with record-breaking temperatures, such as -13°C in Milan and almost -20°C in Emilia (meteolive.it (last access: 26/07/2020) of 11/11/2009, meteo.ansa.it (last access: 26/07/2020) of 17/12/2015, Corriere della Sera of 03/01/1993.

16) 27th December 1996. This cold spell has also affected the UK and France (-7°C in Paris; Le Parisien 03/01/1997) causing the Thames river to freeze in London and 200 fatalities (Jordan-Bychkov and Murphy, 2008). On December 27 snow storms striked the North and the Adriatic side of Italy from Romagna to the South. On December 29, heavy snowfall affected Central Italy and Southern Tuscany in unusual areas (20 cm were recorded on the Lazio coast, 35 cm in Porto Santo Stefano, Aeronautica.Militare (last access: 26/07/2020)). On December 30 snow fell again over the North in Milan, Como, Varese, Pavia

and throughout the whole of Piedmont. A snow storm blew the coastal city of Genoa. Extremely low minimum temperatures affected the areas covered by snow (between -10°C and -15°C in Southern Tuscany and Umbria, Annali Ufficio Idrografico e Mareografico di Pisa 12/1996). The official weather station of the city of Arezzo (Molin Bianco, 248 m a.s.l.) recorded a minimum of -15°C on December 30 (Aeronautica.Militare, last access: 26/07/2020), a monthly record for December from the beginning of records (1957).(La Repubblica 27/12/1996 and 28/12/1996, meteolive.it (last access: 26/07/2020) of 20/10/2017).

17) 31st January 1999. Arctic air reached Italy, particularly affecting the Central and Northern regions, on February 5. The snow affected the entire Po Valley, from Venice to Turin, with accumulations up to 30 cm on the plain. Snow also fell abundantly in the coastal cities of Rimini, Ancona, Grosseto,Genoa, and in the Tuscan cities of Florence and Lucca. A snowstorm struck Viterbo and snow flakes were also observed in Rome with a remarkable -6°C temperature (Annali Ufficio Idrografico e Mareografico di Roma 01-02/1999), which caused the public city fountains to freeze, a rather unusual and damaging phenomenon, given the often ancient origin of the fountains. The temperatures decreased sharply and there were a few days of ice (maximum below zero) in the city. Other notably low temperatures include 3.8°C in Palermo on January 31 (Osservatorio Astronomico di Palermo), -12°C in Norcia (Annali Ufficio Idrografico e Mareografico di Roma) and -21°C in Dobbiaco (1213 m of altitude, (Aeronautica.Militare, last access: 26/07/2020)). The strong Bora wind gusted up to 90 km/h in Trieste on February 4 (Arpa Friuli Venezia Giulia last access: 26/07/2020 02/1999). Snow fell on Sicilian coasts and accumulated up to 5-10 cm in a few hours on the beaches of the Nebrodi areas (Arpa Regione Emilia Romagna Annale Idrologico 01-02/1999, La Repubblica of 24/02/1999, meteoweb.eu (last access: 26/07/2020) of 05/01/2017).

18) 8th December 2001. Before affecting Northern Italy, cold air reached parts of Central-Eastern Europe from Russia. On the evening of December 13, the air mass entered the Po Valley in the form of strong Bora, causing convection accompanied by a blizzard-like snowfall that caused transport, electricity and phone line disruptions, and isolated several small towns in Northern Italy. in Trieste the Bora wind blew at 116km/h with -4°C. In Tarvisio on 15th December the temperature reached -16°C (Arpa Friuli Venezia Giulia last access: 26/07/2020 12/2001). This storm is today remembered as the famous "Blizzard of Saint Lucia", long lived in the memories of the inhabitants of the North, since the blizzard combined heavy snowfalls with damaging winds. On that occasion, the origin of cold air masses was Eastern Europe and Russia. Due to the strong wind, snow fell horizontally and stuck to the walls of buildings, rails and guardrails of highways with heavy transport disruptions and several accidents. The snow accumulation fluctuated between 5 and 25 centimeters on the plains, depending on the area and on exposure to wind, with larger values in Emilia-Romagna: temperatures of -16°C were recorded in Fiorenzuola (422 m of altitude), -7°C in Reggio Emilia and -5°C in Cesena on 17th and 18th December (Arpae.it (last access: 26/07/2020)).(La Repubblica 17/01/2001, meteoweb.eu (last access: 26/07/2020) of 06/12/2011)

19) 20th January 2004. During this event, icy currents flowed from the Northeast towards Northern Italy, with weak snowfalls over Emilia, up to medium-low altitudes. In the following days, however, it snowed again in the North and in the Central regions at lower altitudes: snow reached Tuscany, Lazio, with snow flakes even in Rome. The temperatures in these days of January were particularly low on the north-eastern Alps (-11.2°C Dobbiaco, Protezione Civile Provincia Autonoma di Bolzano 01/2004) and on Central and Southern Italy, where widely negative values were recorded over the usually mild Tyrrhenian plains (-5.2°C at Fiumicino, -6.3°C in Rome and -4°C in Ciampino, Agenzia Regionale Protezione Civile Lazio Annali

Idrologici 01/2004). The whole region of Lazio experienced particularly cold days. The cold also affected Irpinia and Basilicata (with temperatures below zero on the Ionian sea coast, (evalmet.it, last access: 26/07/2020) 01/2004), Molise, Abruzzo and Apulia, where the snow occasionally fell also on the coast. During this event, exceptionally low temperatures were measured in these areas: temperature dropped zero in Foggia, a coastal town in Apulia, (Annali Ufficio Idrografico e Mareografico di Bari 01/2004) and the coastal cities of Naples, Lamezia Terme and Catania. Low daily maximum temperatures (below the 10°C degrees) were recorded also on the Sicilian Tyrrhenian coast, from Messina to Trapani and even in the Syracuse area (Osservatorio delle Acque).(meteogiornale.it (last access: 26/07/2020) of 27/01/2004).

20) 22nd January 2005. Western and Central Europe experienced below average temperatures throughout the winter, with the cold peaking during the month of January. In Northern Italy snow fell abundantly: in Lombardy snow-height reached 30 cm, with peaks up to 40-45 cm, and even the coastal city of Genoa suffered snowfalls (Arpa Liguria Annali Idrologici 01/2004, Aeronautica.Militare (last access: 26/07/2020)). Snow fell also over Marche, Abruzzo, Campania and Basilicata, where inland areas were affected by snowfalls for several days, and accumulations exceeded one meter in Abruzzo, as well as in some areas of Irpinia. There were road disruptions as car drivers were trapped in the snow on highways. Stormy weather also affected other European countries, particularly in France and Spain. In France four avalanches detached from the mountains in Savoy caused many victims in ski resorts.(meteogiornale.it (last access: 26/07/2020) of 23/01/2005; Corriere della Sera of 25/01/2005).

21) 02nd March 2005. A cold and snowy spell hit Central and Southern Italy. Snow fell on the hills of Naples, at medium-low altitude in Calabria, with abundant accumulations on the Central Adriatic coast (from Southern Marche to Molise). A few days later, snowfall spreaded to the North and Tuscany (Servizio Idrologico Regionale Regione Toscana, last access: 26/07/2020). Up to 30 cm of snow fell in Liguria (Arpa Liguria Annali Idrologici 03/2005), on Milan and on most of Lombardy, on the plains of Emilia, on Piedmont, on the North of Tuscany; it snowed in Veneto, whitening Verona, Venice and Rovigo. On March 1, 2005, the lowest temperatures of the winter were recorded, with a country average of -0.5°C, which entered Italy's climatic history. The temperatures in the Alps region reached peaks of -23°C (Marcesina record of -34°C, (Arpav, Arpa Veneto, last access: 26/07/2020)), -20°C at Cimone in the Appennines, -16°C at Terminillo (Agenzia Regionale Protezione Civile Lazio Annali Idrologici 03/2005), -10.8°C in L'Aquila (Annali Idrologici Servizio Idrografico e Mareografico di Pescara 03/2005). Among lowland cities we mention -12°C in Piacenza, -11°C in Novara (Arpa, Piemonte), -10.4°C in Udine (Arpa Friuli Venezia Giulia last access: 26/07/2020) and -9°C in Arezzo (Servizio Idrologico Regionale Regione Toscana, last access: 26/07/2020). (nordestmeteo.it of 02/11/2019; meteogiornale.it (last access: 26/07/2020) of 03/03/2016).

22) 13th December 2007. The peculiarity of this cold spell was the exceptional occurrence of abundant snowfalls, blizzard conditions and an extreme low in temperatures over most of the Sardinian territory, at altitudes on average above 400 m. Also noteworthy are the 2 meters accumulated over an altitude of 1000 m on the slopes of Mount Limbara. Towns were largely unprepared to manage the event. An electricity blackout affected for several hours Cagliari, and schools remained closed for two days. Disruptions were reported in road connections: the main road of the Sardinian network of state highways suffered numerous blocks due to some trucks blocking the roads. In Nuoro, the snowfall exceeded 50 cm, breaking the record (Annali Idrologici della Sardegna 12/2007). A strong wind and rough seas were observed on the coasts. Low temperatures affected also the Central and Southern Italy: -10°C and icy roads were reported in Calabria, snowfalls in Molise as well as in the hinterland

of Bari, Foggia and Taranto (Annali Ufficio Idrografico e Mareografico di Bari 12/2007), in Basilicata (Agenzia Regionale Protezione Civile Basilicata Annali Idrologici 12/2007); below-zero temperatures were recorded on the Ionian coast (evalmet.it (last access: 26/07/2020) 12/2007).(La Repubblica of 13/12/2007, meteolive.it (last access: 26/07/2020) of 19/12/2007).

23) 17th December 2009. Most of the Central and Northern Europe has been struck by this cold spell. On December 19, snow fell over most of Northern Italy, and it was especially copious in Tuscany (Servizio Idrologico Regionale Regione Toscana, last access: 26/07/2020). A strong glazed frost occurred in Emilia and Liguria (Arpae.it (last access: 26/07/2020)). Extreme low temperatures were recorded in some lowland locations (especially on December 20) in Friuli Venezia Giulia (Arpa Friuli Venezia Giulia last access: 26/07/2020): Udine Rivolto -18°C, Pordenone -12.4 °C, Cervignano del Friuli -17.3 °C, in coastal locations as Lignano -6.3°C, in some alpine valleys as Tarvisio (754 m above sea level) -18.3°C, Fusine (850 m a.s.l.) -22°C. (La Repubblica 19/12/2009 ; meteogiornale.it (last access: 26/07/2020) of 19/12/2014; Il Quotidiano 19/12/2009).

24) 12th February 2010. Snowfalls affected several regions, from Emilia Romagna to Calabria, Marche and Sardinia (Arpae.it (last access: 26/07/2020), Annali Idrologici della Sardegna 02/2010). Bologna airport was closed for several hours: 17 flights were cancelled, 15 diverted. The heaviest snowfall in Rome (ARSIAL: Agenzia Regionale per lo Sviluppo e l'Innovazione dell'Agricoltura del Lazio, last access: 26/07/2020) since February 1986 was recorded, causing transportation disruptions, with many roads were closed both inside and outside the city. Many interventions were required to rescue motorists involved in collisions and stuck on the highway between the Marche and Romagna (the distribution of comfort items for at least 2000 people stuck in cars was necessary). A blizzard hit the Sila region, where the schools were closed for a few days. (roma artigiana.it (last access: 26/07/2020) 26/02/2018, La Stampa of 12/02/2010; La Repubblica 12/02/2010; ansa.it (last access: 26/07/2020) of 12/02/2010).

25) 11th December 2010. An Arctic air mass reached the Eastern side of Italy, giving rise to intense snowfalls on the Adriatic and Thyrrenian coasts (especially the coasts surrounding the city of Livorno). Snow also whitened Tuscany (25 cm fell in Florence), Umbria and part of Lazio, with snow flakes observed in Rome. An exceptional snowstorm hit Ancona and the surrounding areas between December 14 and 15. There, the Adriatic Effect Snow contributed to reach snow heights up to 30 cm in the Chieti area and 40 cm in Lanciano. The temperatures were extremely cold over most of Italy. Malpensa Milan airport measured a minimum temperature of -14°C and Rome reached -7.7°C, a record value for the month of December (ARSIAL: Agenzia Regionale per lo Sviluppo e l'Innovazione dell'Agricoltura del Lazio, last access: 26/07/2020). Very low temperatures were also recorded on 17th December in Forlì (-6°C), in Parma (-7.5°C, Arpae.it (last access: 26/07/2020)), as well as in Ancona -6.8°C (Annali Idrologici, Centro Funzionale Mutlirischi per la Meteorologia, l'Idrologia e la Sismologia Regione Marche 12/2010) and in Firenze with its -7.3°C (Servizio Idrologico Regionale Regione Toscana, last access: 26/07/2020), in Isernia -11.8°C , in Salerno (Tirrenean coast) -7.2°C (Annali Idrologici, Centro Funzionale Mutlirischi per la Meteorologia, l'Idrologia e la Sismologia Regione Capania)(Il Messaggero 17/12/2010, 3bmeteo.com (last access: 26/07/2020) of 19/12/2015, cemcer.it (last access: 26/07/2020) of 17/12/2015, Randi and Ghiselli (2013)).

26) 02nd February 2012. The February 2012 cold spell affected a large part of Europe and spread down to North Africa in the period between 27th January and 20th February 2012, causing over 650 deaths in the concerned areas. The event was characterized by extremely low temperatures, especially over Eastern Europe, with an absolute minimum of -42.7°C in Finland, and

heavy snowfall on the remaining European countries (Assessment of the observed extreme conditions during late boreal winter 2011/2012. WMO, 2015). On February 4, snow fell even in Algiers with an accumulation of about 20 cm and the cold air brought snow even in the Sahara Desert (ansamed.info (last access: 26/07/2020) of 08/02/2012). In Italy the cold spell caused serious hardships and at least 57 victims (La Repubblica 12/02/2012). From the end of January, a stream of Arctic air reached the peninsula. At first, only the northern regions were affected (e.g. Alessandria recorded -20°C, Milan -14.5°C), but the cold later spreaded to the Central and Southern regions (Annali Idrologici, Centro Meteorologico Lombardo 02/2012). Snow fell on most of Italy, especially in Emilia-Romagna and in the provinces of Pesaro-Urbino, Ancona, Macerata and Fermo in the Central regions. A daily low of -7.6°C was recorded in Bologna on 6th February, -10.2°C in Parma, -6.2°C in Rimini, (Arpae.it, last access: 26/07/2020). Snow fell over several areas of Southern Italy, such as Basilicata and Calabria, and on the Monte Pellegrino in Palermo on the 14th February (Agenzia Regionale Protezione Civile Basilicata Annali Idrologici 2012; palermotoday.it (last access: 26/07/2020) of 14/02/2012). The hinterland and the rest of the region were affected by accumulations beyond 20-30 cm. (La Repubblica 12/02/2012), Annali Idrologici, Centro Meteorologico Lombardo 15/02/2012).

27) 7th February 2013. This cold spell consisted of a polar trough spreading towards the Mediterranean region: the -12°C 850 hPa isotherm reached Central Europe and a 850 hPa temperature of -6.7°C was measured at midnight on February 10 in the Linate Milan airport radiosounding (Wetterzentrale.de (last access: 26/07/2020)). The minimum temperatures of February 10 were very cold in the lower Ticino valley, and February 11th was a snowy day on most of the Northern Italian plains, with diurnal temperatures around zero degrees. This has been an important snow event on the Po Valley: 20 cm accumulated in Milan during 36 hours of snowfall, and the largest accumulations were found in the Brianza area North of Milan, where peaks exceeding 35 cm were recorded Annali Idrologici, Centro Meteorologico Lombardo. Heavy snowfalls were reported in Emilia, in the Lombardy plain, Veneto, lower Trentino and Friuli. Accumulations reached up to 10-15 cm snow-height between Emilia, Southern Veneto, and Southern Lombardy. Stormy weather also affected the rest of Italy, but snow fell only at mountain altitudes, with some episodes at lower altitudes especially in Tuscany. Annali Idrologici, Centro Meteorologico Lombardo 29/02/2016, Arpae.it (last access: 26/07/2020); Arpav (Arpa Veneto, last access: 26/07/2020), Servizio Idrologico Regionale Regione Toscana, last access: 26/07/2020, meteogiornale.it (last access: 26/07/2020) of 11/02/2018 milanotoday.it (last access: 26/07/2020) 18/12/2013; Milano.Repubblica (Milano Repubblica 11/02/2013)).

28) 28th December 2014. This cold spell affected the South of Italy with locally exceptional snowfalls, especially in Sicily and Apulia, the latter recording important accumulations on the plains and coasts. Snow has also appeared in Naples and on the Amalfi coast. Snowfalls affected Sicilian coasts including the city of Messina, the hills and the hinterland of Palermo, with large accumulations, and Syracuse. The event was modest on Catania, with accumulations only on the hills of the city. The extreme South-Eastern tip of Sicily experienced snowfall on New Year's Eve, an extremely rare event, as these southernmost areas of the country had not received snow since January 1905. Historic snowfall were also recorded in Pachino, a city famous for the production of a special type of cherry tomatoes. Snowfall also affected Sicilian towns of the Ionian side, like Avola and Noto. This cold spell was extraordinary also in the south of Sardinia, where Cagliari and surrounding areas were covered by snow (Arpa Sardegna, Analisi Agrometeorologica e Climatologica della Sardegna. 2014-2015). (Annali Idrologici 12/2014, Osservatorio delle Acque, La Repubblica 27/12/2014).

29) 5th February 2015. Italy was affected by stormy and snowy conditions. It snowed extensively in Piedmont as well as in Liguria, a region also affected by strong winds. Snow fell at low altitudes and in the lowlands in the Northern Italy and in part of the Centeral Italy. During this event, due to the strong winds, Sicily was isolated and the connections with the smaller islands were interrupted. In the surrounding of Etna, snow, wind gusts and ice caused blizzard conditions. In Enna temperature dropped to -4.2°C (Annali Idrologici 02/2015, Osservatorio delle Acque). The most difficult situation was observed in Ustica, as ferries could not reach the island for 12 days, and essential medicines were delivered in dangerous operations by helicopters. Many flights were canceled at Sicilian airports. Many roads and highways remained closed as the snow cover exceeded 50 centimeters in some areas. On the 9th February, ANAS (Azienda nazionale autonoma delle strade) reported that heavy snowfall causing traffic jams in the provinces of L'Aquila and Teramo. In Northern Italy, snow caused an electrical blackout: numerous municipalities in the Bologna area, and many others in the region, experienced a blackout in light, heating and water supply, as well as malfunctions on the telephone network and the Internet. On February 7 a big snowfall involved the city of Parma and the whole Emilia-Romagna region (-7.4°C on 9th February, Arpae.it (last access: 26/07/2020)), with road accidents and problems in the supply of electricity for about 12 thousand customers in the Municipality of Parma. (livesicilia.it (last access: 26/07/2020) of 05/02/2015; today.it (last access: 26/07/2020) 09/02/2015; La Repubblica Bologna 10/02/2015).

30) 16th January 2016. On January 17 cold air flowed from Russia, over-passed the barrier of the Alps and reached the Apennine chain. Due to the strong winds and rough sea, the Eolian islands were isolated and the highest peaks of the islands (Stromboli and Salina) were whitewashed. Storm surges stroke the Sicilian North coast (Palermo Osservatorio delle Acque). In Molise, snow covered almost the entire region, even at low altitudes. The city centre of Lanciano (Regione Abruzzo Dipartimeto Politiche dello Sviluppo Rurale e dell'Ambiente) was covered by up to 25 cm of snow, and 50 cm to 60 cm snow height was also measured in the bordering side of the coasts. Snow fell throughout Basilicata (Agenzia Regionale Protezione Civile Basilicata Annali Idrologici 01/2016) and temperatures reached -8°C. Whitewashed peaks appeared at lower altitudes, as well as the Aspromonte. Accumulations reached up to 20 cm on some area of Cosenza (150 m above sea level) and over 30 cm on the highest hills surrounding the city. Snow caused many issues, mainly to viability, with traffic jams on the Salerno-Reggio Calabria highway. Calabria has been the area most affected by the snow, even recording some casualties.(meteopalermo.it (last access: 26/07/2020) of 19/01/2016, La Repubblica 17/01/2016 , today.it (last access: 26/07/2020) of 19/01/2016)

31) 5th January 2017. From the 5th to the 21st January 2017, a cold spell affected most of Eastern and Central Europe and part of Southern Europe, causing the death of at least 60 people. The cold and snowfalls mainly affected Central and Southern Italy. The regions most affected by this cold spell were the Adriatic ones, namely Marche, Abruzzo, Molise, Puglia and Basilicata. Snow reached almost all coastal areas of these regions, with snow totals up to 40 cm. On January 8, the beach of Porto Cesareo (LE) in Apulia was covered at some points with accumulations of 22-23 cm, resulting as the third most snowy Italian beach since 2000. The situation was worse in inland areas, where snow often exceeded 2 meters height. A strong snowstorm affected the entire Marsicano sector (Abruzzo) with temperatures ranging between -10°C and -13°C, and final accumulations near one meter and temperatures below -20°C below 1300 meters of altitude (Regione Abruzzo, Servizio Presidi Tecnici di Supporto al Settore Agricolo.). On the 9th January, the combination of heavy snowfall and a seismic swarm in Central Italy triggered a disastrous avalanche that hit the town of Rigopiano in Abruzzo: a landslide swept and destroyed a hotel, causing the

death of several people that were blocked there due to the exceptional snowfall, which also considerably complicated rescue operations in this region (Corriere della Sera of 19/01/2017). (Aljazeera of 07/01/2017 of 07/01/2017, severe weather.eu (last access: 26/07/2020) 05/01/2017 and of 08/01/2017, La Repubblica 05/01/2017 05/01/2017).

32) 18th February 2018. The cold spell affected Europe between the end of February 2018 and the beginning of March. The major anomalies concerned the Central and Northern sector of Europe with temperatures between 5°C and 9°C below the reference average 1971-2000, but consistent anomalies were however recorded also over Italy. The cold was felt more intensely in the Central and Northern and marginally in the far South Italy and on Sicily. In the Northern regions, temperature values were up to 8-9°C below seasonal averages. Rome experienced a moderate snowfall (3-4 cm of snow), which caused temporary disruptions in ground transportation. The last snowfall in Rome, in chronological order, was February 2012, when the city was covered with snow for the first time after many years. In Cagliari, Mistral (North-Westerly) wind was extremely strong, with gusts up to 100 km/h, creating disruptions in the maritime connections between the Sardinia and the rest of the continent. Gale force winds were recorded all over the regions, for example wind exceeded 70 km/h in Capo Caccia, on the North Coast, and 80km/h in Capo Carbonara, on the South coast (Decimomannu, Aeronautica.Militare (last access: 26/07/2020)). Snow covered the slopes of the Riviera di Ponente, and fell in Rome, Naples (the last snowing event on 1956), Olbia and Bari Arpa (Puglia). The minimum temperatures of February 27-28 were the lowest in the last 20-30 years above 1500 m at many locations in the Alps, with up to -25°C recorded at 2500 m near Bolzano (Protezione Civile Provincia Autonoma di Bolzano). A second pulse of cold air mass reached Italy through the Carso in the early hours of February 25, spreading throughout Northern Italy during the daytime, along with winds and irregular snowfalls on the plains between Emilia and Piedmont. New monthly records for February were observed in Bologna (-9.1°C), in Rome-Ciampino (-6.2°C Arpae.it (last access: 26/07/2020), second lowest after the -6.5°C reached on 2nd March 1963), -1.1°C in Brindisi (15 m, on 11th March 1956 it reached -4.2°C)(Aeronautica.Militare, last access: 26/07/2020). (Il Foglio 26/02/2017; La Gazzetta di Parma 14/02/2018; La Gazzetta del Serchio 22/02/2018, nimbus.it (last access: 26/07/2020) 02/03/2018).